MICROCOPY RESOLUTION TEST CHART

NATIONAL BUREAU OF STANDARDS-1963-A

⊞TRI

AD-A184 823

(12)

NDE OF ADHESIVE BONDS

PHASE I

Cecil M. Teller and K. Jerome Diercks

TEXAS RESEARCH INSTITUTE, Inc.

9063 Bee Caves Rd.

Austin, Texas 78733-6201

DTIC
SELECTED
SEP 1 7 1987
S D

11 August 1987

Prepared for

87   9 14 006

REPORT DOCUMENTATION PAGE		READ INSTRUCTIONS BEFORE COMPLETING FORM
1. REPORT NUMBER	2. GOVT ACCESSION NO. *ADA184823*	3. RECIPIENT'S CATALOG NUMBER
4. TITLE (and Subtitle) NDE OF ADHESIVE BONDS PHASE I		5. TYPE OF REPORT & PERIOD COVERED Final; 9/15/86-5/31/87
		6. PERFORMING ORG. REPORT NUMBER 86194:CMT
7. AUTHOR(s) Cecil M. Teller and K. Jerome Diercks		8. CONTRACT OR GRANT NUMBER(s) N00014-86-C-0631
9. PERFORMING ORGANIZATION NAME AND ADDRESS Texas Research Institute, Inc. 9063 Bee Caves Rd. Austin, TX 78733		10. PROGRAM ELEMENT, PROJECT, TASK AREA & WORK UNIT NUMBERS SBIR
11. CONTROLLING OFFICE NAME AND ADDRESS Office of Naval Research 800 N. Quincy Street Arlington, VA 22217		12. REPORT DATE 11 August 1987
		13. NUMBER OF PAGES 51
14. MONITORING AGENCY NAME & ADDRESS(if different from Controlling Office)		15. SECURITY CLASS. (of this report) UNCLASSIFIED
		15a. DECLASSIFICATION/DOWNGRADING SCHEDULE

16. DISTRIBUTION STATEMENT (of this Report)

Approved for Public Release; Distribution Is Unlimited

17. DISTRIBUTION STATEMENT (of the abstract entered in Block 20, if different from Report)

18. SUPPLEMENTARY NOTES

19. KEY WORDS (Continue on reverse side if necessary and identify by block number)

Nondestructive Evaluation	NDE
Adhesive Bonds	Rubber-to-Metal Bonds
Leaky Lamb Waves	

20. ABSTRACT (Continue on reverse side if necessary and identify by block number)

This report describes the results of a successful effort to demonstrate the feasibility of using leaky Lamb waves to detect and delineate flaws in the bond surface of metal/rubber laminates, even when the adherends remain in intimate contact. It is shown that the leaky Lamb wave method can detect and image a poorly bonded area in a bonded surface when a conventional pulse-echo method failed even to detect the flaw. A new technique was implemented for preparing partially bonded surfaces

DD FORM 1473 EDITION OF 1 NOV 65 IS OBSOLETE

20. ABSTRACT (cont.)

by varying the percentage of adhesive coverage, and results are provided
that illustrate the sensitivity of the leaky Lamb wave method in detect-
ing different surfaces prepared by this technique. An analytical model
of the leaky Lamb wave phenomenon in homogeneous, isotropic metal/rubber
laminates is described. Numerical results for a metal/rubber laminate
immersed in water are included.

TABLE OF CONTENTS

Accesion For

NTIS CRA&I	☑
DTIC TAB	☐
Unannounced	☐
Justification	

QUALITY INSPECTED 2

By ....
Distribution /

Availability Codes

| Dist | Avail and / or Special |

A-1

1

LIST OF FIGURES

List of Figures, Cont'd.

SUMMARY

Texas Research Institute, Inc. (TRI), under ONR/SBIR Contract No. N00014-86-C-0631, investigated and demonstrated the feasibility of using ultrasonic leaky Lamb waves (LLW) to detect and delineate flaws in bonded metal/rubber structures. Technical consulting support for this work was provided by Dr. Y. Bar-Cohen, Douglas Aircraft Co. (DAC), Long Beach, CA. The specific focus of the project was rubber/metal laminates where the layers, though not bonded, remain in intimate contact. Conventional ultrasonic techniques have shown little-or-no success on this problem. The applicability of the LLW method to evaluation of bond quality, where bond quality is here defined as the degree of adhesive coverage, was also examined.

A long range goal of this work is to develop and engineer a nondestructive method for evaluating the bond state in the rubber annulus of a sonar transducer head mass assembly (HMA), for example, the TR-317( ), on a production-line basis. The work reported here employed metal/rubber structures dimensionally similar to the TR-317( ) HMA, with programmed flaws in the bond surface, or with a specifiable degree of adhesive coverage. The results demonstrate the feasibility of using leaky Lamb waves to detect and evaluate flaws in metal/rubber bond surfaces and the increased sensitivity of the LLW method over a conventional pulse-echo method. Flaws in bonded surfaces were reliably detected and delineated using LLW where a conventional pulse-echo method was unable even to detect the flaws.

TRI prepared partially bonded surfaces in metal/rubber laminates by applying adhesive over a geometrically defined mask to yield a known percentage of adhesive coverage. The LLW method readily discriminated a fully bonded surface from a partially bonded surface prepared in this way.

Various procedural and signal processing techniques were devised to either reduce the deleterious effects of material anisotropy and/or inhomogeneity on signal-to-background ratio or to enhance signal detection in their presence. For example, the background level is reduced, i.e., the signal-to-background ratio is increased, by orienting the transmit-receive plane parallel to the grain axis of the material. Scanning at several Lamb mode frequencies and summing the scans increases the signal-to-background ratio by reducing the background level in a manner akin to the averaging of multiple measurements of signal-in-noise.

The work performed under this Phase I SBIR contract showed the _feasibility_ of using the LLW method to detect and evaluate flaws in bonded metal/rubber structures. Several problem areas--e.g., interaction of measurement parameters, data display formats--in need of more comprehensive examination were identified. These, and methods to examine and assess them, were detailed in a proposal to ONR for further research and development of LLW technology under Phase II SBIR funding.

1.0 INTRODUCTION

Adhesive bonding provides a means for transferring load between various structural components of a bonded assembly. A proper transfer can be accomplished only through a continuous medium between the adherends. Furthermore, the adhesive must have sufficiently high strength to allow the performance of the structure to meet design requirements. The strength of a bonded joint depends on many factors, including proper curing, porosity, proper surface preparation, type of adhesive, elastic properties of the adhesive and thickness.

Of particular interest to the Navy are adhesive bonds formed between rubber and metallic adherends. Rubbers and other elastomeric materials are used to protect and seal various components of hardware employed in or operated at sea, specifically, underwater transducers, connectors, etc. A reliable long-term bond between the elastomeric seal and the metallic structural member is essential for effective and efficient performance of the device. For example, the electroacoustic components of sonar transducers are protected from the seawater environment by a rubber or urethane seal that functions both as a water barrier and as an acoustic window. A seal that leaks in-service, as a consequence of a poor or improper bond, will degrade system and therefore mission performance. The rubber-to-metal bonding problem is thus a very important subset of the generic bonded joint problem.

Conditions for obtaining a quality bond are not easily reproduced. Bond quality may be seriously affected by trace amounts of foreign substances that cause weak boundary layers. Weak boundary layers may be formed when the bond is initially made or may be created under use conditions by migration of species

that were present initially but subsequently were dispersed throughout the interphase, or that invaded the bondline from the surrounding environment. However, when the correct choice of adhesive is made and proper bonding conditions are achieved, very satisfactory and environmentally resistant bonds result.

The problem is to know with reasonably high confidence when satisfactory bonds have been produced. In practice, the Navy relies on process control and a relatively high level of destructive testing for quality assurance. Frequently, however, poorly bonded hardware is accepted. Thus, there is a major need for nondestructive (non-invasive) evaluation methods for inspecting bonded joints in newly fabricated components. Generally, these methods should also be applicable to evaluating components that are or have been in service. Further, a successful nondestructive bond evaluation method should significantly benefit development of new bonding techniques or materials.

The literature on nondestructive evaluation (NDE) of adhesive bonds reveals that gross defects can be detected by several different methods, e.g., ultrasonic resonance, pulse-echo ultrasonics, holography, etc. However, successful detection and evaluation of bond flaws in areas where the adherends are in intimate contact has proven elusive, although many different methods have been proposed and tried.

Chimenti, Bar-Cohen and others, have reported success in detecting and imaging bond flaws in fiber-composite laminates using leaky Lamb waves [1-6]. Prior to the present contract, TRI had submitted a bonded rubber/metal laminate to Bar-Cohen at DAC for examination. This specimen was a 15 cm (6 in.) square, 0.16 cm (0.62 in.) thick, flat steel plate with a 0.16 cm (0.62 in.) thick layer of neoprene bonded to it. A 1.3 cm (0.5 in.) square debond was programmed in

4

the center of the adhesive layer. Neither TRI nor DAC was successful in detecting the debond using conventional ultrasonic methods. Bar-Cohen, however, was able not only to detect but also to image the debond using the LLW method. His results are shown in Figure 1. Based on this and other encouraging, but equally preliminary, results, TRI proposed to explore the applicability, and limitations, of the LLW method to assessment of bonded rubber-to-metal structures of importance to the Navy, particularly wet-end sonar hardware.

2.0 PHASE I GOALS AND TECHNICAL OBJECTIVES

The overall goal of the research and development effort in LLW technology is to implement a nondestructive evaluation (NDE) method that can determine whether a durable adhesive bond has been formed in rubber-to-metal joints and whether a bond that has been exposed to use conditions maintains its integrity.

The specific goals of this Phase I effort were to identify, describe and evaluate the conditions and limitations for exciting and detecting Lamb waves in rubber-to-metal laminates, and to demonstrate the feasibility of using LLW to detect and discriminate bond flaws or bond states in rubber/metal structures of importance to the Navy.

The specific technical objectives of the Phase I effort were:

1. to examine and evaluate any thickness-to-wavelength limitations for exciting Lamb waves in metallic adherends and for assessing the status of the bond joint; this would be accomplished by varying the thicknesses of the adherends and the adhesive layer as well as the insonifying signal frequency,

2. to assess the applicability of existing theories of wave excitation and propagation in layered media to bonded rubber-to-metal laminates,
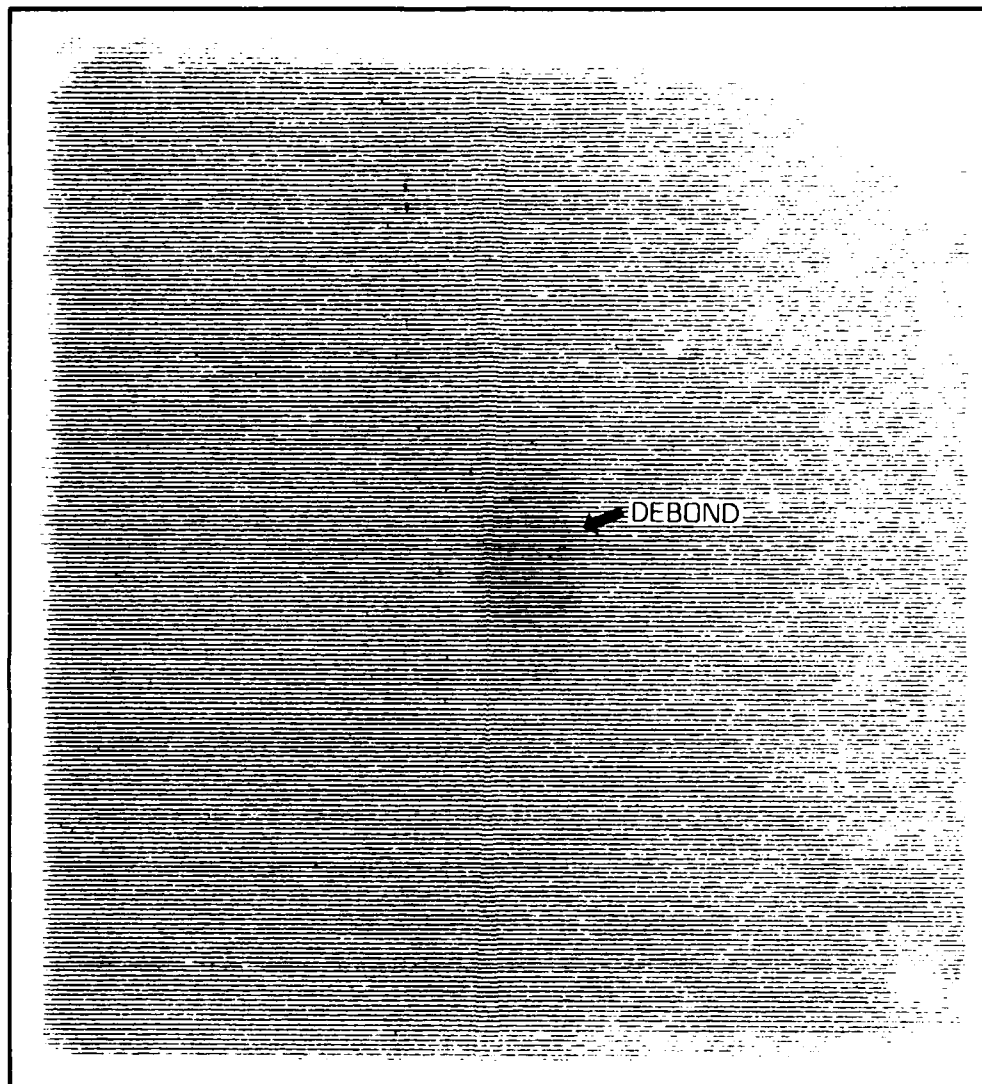
Figure 1

C-scan image of a 1.27 cm (0.50 in.) square debond in the adhesive layer
of a metal/rubber laminate obtained using the LLW method.

0.16 cm (0.06 in.) thick metal/rubber layers   Frequency: 4.49 MHz

3.   to implement a quantifiable method for producing different degrees of adhesion in rubber/metal laminates, and

4.   to assess the sensitivity of the LLW method in detecting and discriminating variations and changes in the bond caused by improper preparation or by degradation through use; this would be accomplished by mechanical stressing of the bond joint to increase the debonding stresses as well as accelerated aging of specimens.

Early measurements showed that Lamb waves could readily be excited in metal/rubber structures with adherend thicknesses relevant to Navy applications (see Section 4.2). Therefore, in consideration of the limited time and funds available, the work under Objective 1. was pursued only to this extent. Also, time and funding did not permit employment of mechanical stressing or the use of accelerated aging to degrade the bond joint as proposed under Objective 4.

3.0 THE LEAKY LAMB WAVE PHENOMENON

Metallic and composite plates in the thickness range from about 0.02 to 2.5 cm (about 0.01 to 1 in.) support the excitation of Lamb waves within the range of frequencies, 1 to 10 MHz, commonly employed in ultrasonic NDE. Physically, a Lamb wave is a vertically polarized travelling plate wave [7]. It is excited under immersion conditions by an external compressional wave impinging on the surface of the plate at an oblique angle of incidence. Mode conversion occurs at the locus of insonification, and transverse and compressional waves are generated in the plate. These propagate in the plate at their respective velocities, each experiencing refraction and multiple reflections at the plate boundaries. The modal pattern of plate vibration that results is the Lamb or plate wave. The character of the Lamb wave may be

symmetric, i.e., the surfaces of the plate move simultaneously in opposite directions with equal amplitude about the undistorted central plane (see Figure 2(a)), or it may be antisymmetric, i.e., the surfaces move in the same direction with equal amplitudes parallel to the distorted central plane (see Figure 2(b)). If the relative acoustic impedance of the surrounding medium is similar to that of the plate, the plate will reradiate, or leak, energy into the medium, hence the name leaky Lamb wave (LLW). The direction (angle) of radiation is determined principally by the Lamb wave phase velocity and Snell's Law.

The modal pattern established in the plate depends on the driving frequency, the angle of insonification, the plate thickness, and, if there is more than one layer, e.g., a laminate, the acoustic characteristics of the interfacial boundaries. For fixed geometry and fixed frequency, the modal excitation will depend on the characteristics and nature of the interfacial boundaries. This is the basis of the LLW method for assessing rubber-to-metal bond surfaces.

If a bonded rubber-to-metal structure is immersed in a fluid such as water, and the metal surface is insonified at an oblique angle of incidence (see Figure 3), part of the energy in the incident wave will be reflected back into the surrounding water and part will be coupled into the metal plate and will propagate therein. A small part will propagate across the metal-to-rubber boundary into the rubber layer and be dissipated there. If the wavelength is commensurate with the plate thickness, the energy in the plate will generate a Lamb wave, part of which reradiates or leaks into the surrounding water. Within the beam of the reflected wave, the reflected and the reradiated waves will interfere (see Figure 3). Along an axis where the two wave paths differ by one-half wavelength, they will destructively interfere to yield a signal null.
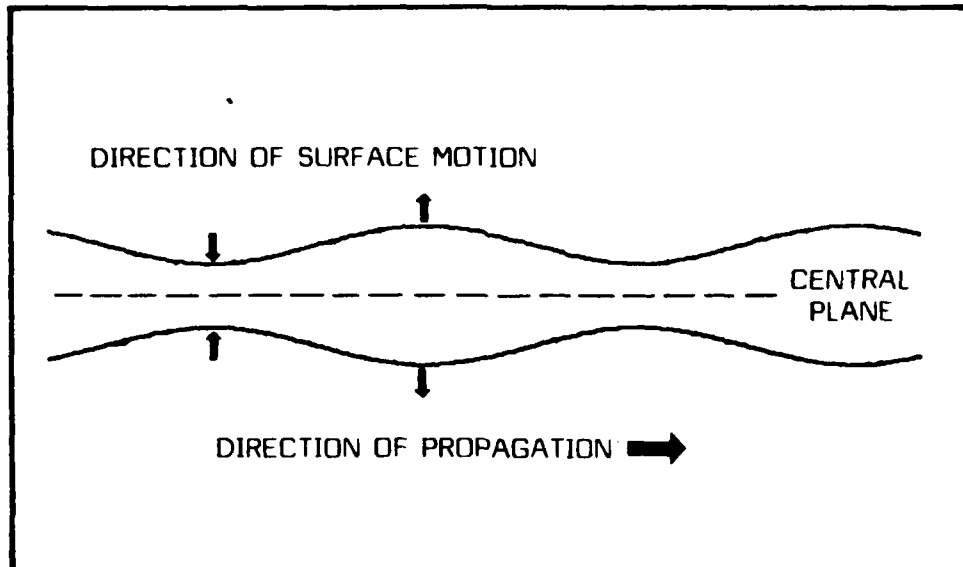
(a) SYMMETRIC PLATE WAVE
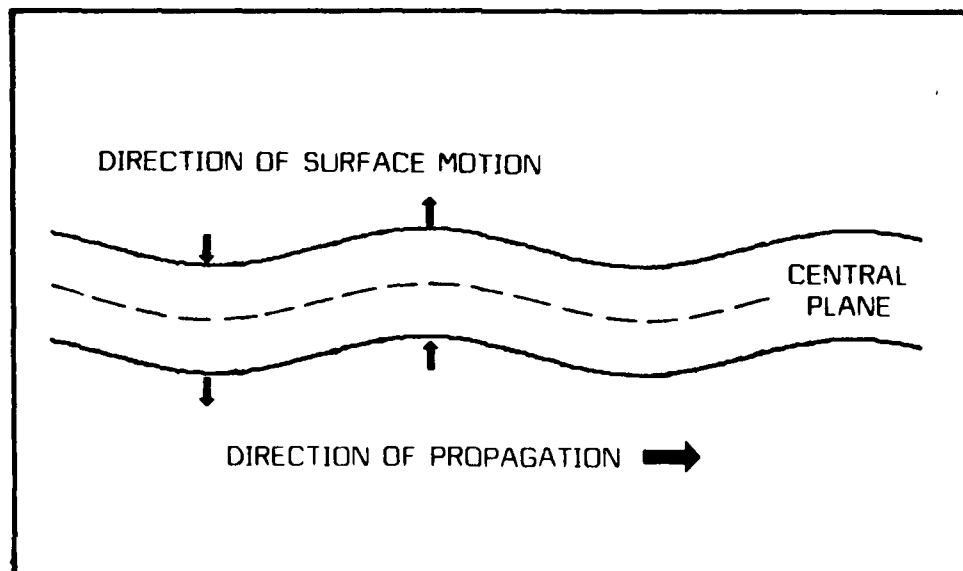
(b) ANTISYMMETRIC PLATE WAVE

Figure 2

Cross-sectional diagrams of symmetric and antisymmetric plate waves.
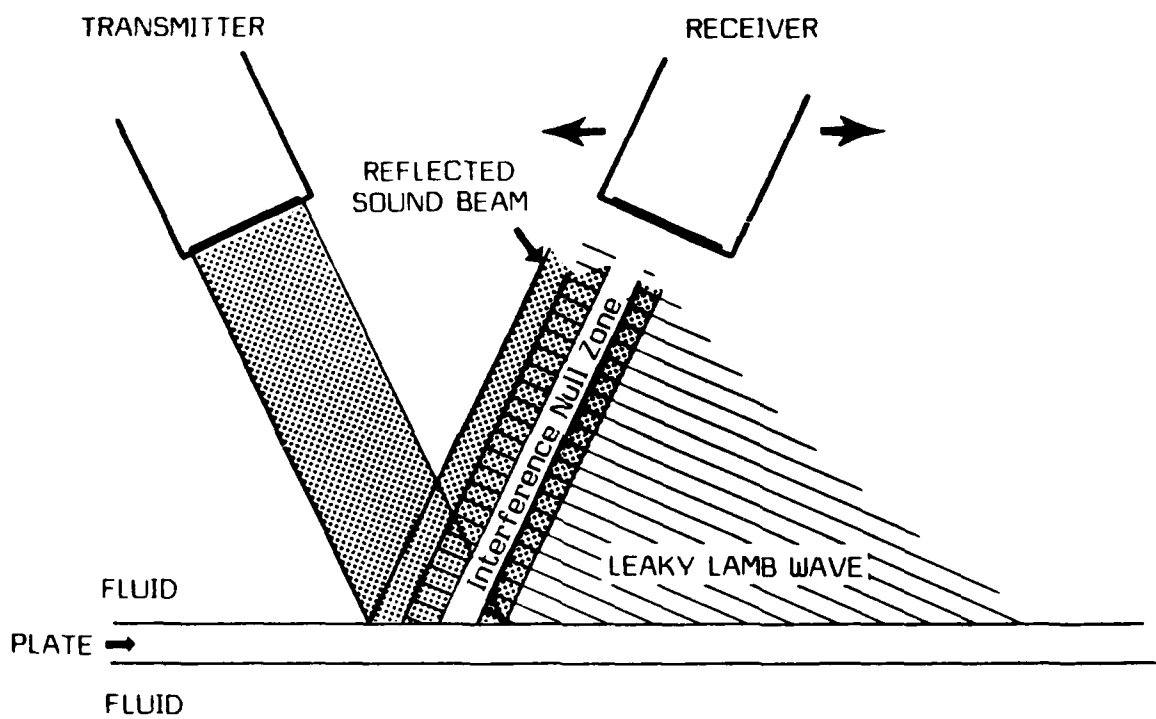
Figure 3

Diagrammatic description of leaky Lamb wave interference field.
(After Chimenti [3].)

Detection of this null indicates that a leaky Lamb wave has been excited in the bonded structure.

There is extensive literature relating to acoustic reflection at planar interfaces and by layered media. Interest in exploiting Rayleigh and Lamb waves for nondestructive evaluation of interfacial bonds began with the reporting by Goos and Haenchen [8] of an apparent departure from expected geometric reflection of a light beam at the interface between transparent media. Shortly thereafter, Schoch predicted [9] and subsequently verified [10] a similar effect for an acoustic beam impinging on a liquid/solid interface. Schoch's work did not, however, account for the observed null in the reflected field and the trailing or smearing of the field (see Figure 3). This deficiency was overcome by Bertoni and Tamir [11] who did an analysis in the complex plane to derive approximate, but reasonable, reflection coefficients and reflected sound intensity profiles for a liquid/solid interface. Mayer et al [7,12,13], and more recently Mal (see below), have examined the problem of a plate immersed in a liquid, i.e., a liquid/solid/liquid layered system.

A thorough analysis of Lamb wave excitation in planar laminates composed of homogeneous, isotropic materials immersed in a fluid has recently been carried out by Mal and his associates at UCLA in collaboration with Bar-Cohen [14-18]. The main features of their theory are presented below.

The geometry of the problem is diagrammed in Figure 4. The laminate, comprising N-1 layers, may be totally immersed, in which case the upper (Z_o) and lower (Z_{N-1}) boundaries are in contact with the liquid, or the structure may be airbacked with only the upper surface in contact with the liquid. The surface is insonified at an angle to the normal. Propagation of the Lamb wave is in the positive x-direction. Phenomenologically, $R(\theta,f)$ is the magnitude of the leaky Lamb wave at frequency f radiated in the θ direction. Analytically, R is a reflection coefficient.
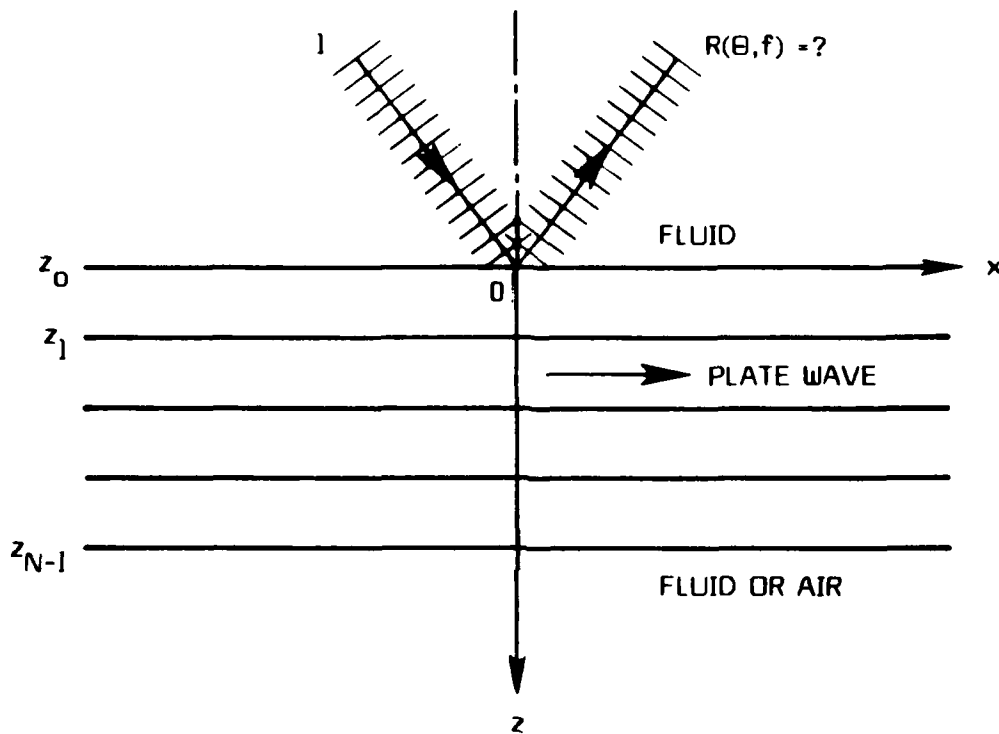
11

Figure 4

Diagram of layered model.
(After Mal [14].)

The parameters used in the analysis are:

$N-1$ = number of layers

α_n = longitudinal (P) wave speed in nth layer (mm/μsec)

β_n = transverse (S) wave speed in nth layer (mm/μsec)

ρ_n = density of nth layer (gm/cc)

z_n = depth of nth interface (mm)

α_o = acoustic wave speed in top fluid

α_N = acoustic wave speed in bottom fluid

ρ_o = density of top fluid

ρ_N = density of bottom fluid

ω = circular frequency of incident wave

f = $\omega/2\pi$ = frequency in MHz

θ = incident angle

k_{α_j} = P-wave number, j = 0, 1, $\cdots$, N

k_{β_j} = S-wave number, j = 1, 2, $\cdots$, N-1

For solid materials the governing equations are:

Displacement components: $u(x,z,\omega)$, $w(x,z,\omega)$

Stress components: σ_{xx}, σ_{zz} σ_{xz}

Potential functions: $\phi(x,z,\omega)$, $\psi(x,z,\omega)$

Equations:

$$\nabla^2\phi + k_\alpha^2\,\phi = 0$$

$$\nabla^2\psi + k_\beta^2\,\psi = 0$$

The potentials have the form

$$\phi = \Phi(z,\omega)e^{i(kx-\omega t)},$$
$$\psi = \Psi(z,\omega)e^{i(kx-\omega t)}, \tag{1}$$

13

where

$$i = \sqrt{-1}$$

$$k = k_{\alpha_o} \sin \theta.$$

Then

$$\phi = a^+ e^{i\eta_\alpha (z-\zeta)} + a^- e^{-i\eta_\alpha (z-\zeta)}$$

$$\psi = b^+ e^{i\eta_\beta (z-\zeta)} + b^- e^{-i\eta_\beta (z-\zeta)}, \tag{2}$$

where

$$\eta_\alpha = (k_\alpha^2 - k^2)^{1/2}, \quad k < k_\alpha \text{ (homogeneous wave)},$$

$$= i(k^2 - k_\alpha^2)^{1/2}, \quad k > k_\alpha \text{ (inhomogeneous wave)},$$

and similarly for η_β.

In Equation (2) a^+ is the amplitude of "downgoing" P-waves, a^- is the amplitude of "upgoing" P-waves and $b^\pm$ are analogous amplitudes for the S-wave.

$U(z,\omega)$, $W(z,\omega)$, $P(z,\omega)$, $T(z,\omega)$ are defined by the following equations:

$$u = U e^{i(kx-\omega t)}$$

$$w = W e^{i(kx-\omega t)}$$

$$\sigma_{zz} = P e^{i(kx-\omega t)} \tag{3}$$

$$\sigma_{xz} = T e^{i(kx-\omega t)}.$$

Then

$$U = ik\phi(z) - \psi'(z),$$

$$W = \phi'(z) + ik\psi(z), \tag{4}$$

$$P = \rho\beta^2 [(2k^2 - k_2^2)\phi(z) + 2ik\psi'(z)], \text{ and}$$

$$T = \rho\beta^2 [2ik\phi'(z) - (2k^2 - k_2^2)\psi(z)].$$

14

For the fluid material, $\phi=0$ and $\beta=0$ so that

$$U = ik\phi(z),$$
$$W = \phi'(z),$$
$$P = -\rho\omega^2\phi, \text{ and} \tag{5}$$
$$T = 0.$$

Perfect bonding between layers means that U, W, P, T are continuous for all z. (An example of imperfect bonding would be W and P continuous, T=0, with radiation occurring at large z.)

For a multilayered laminate, assume that

$$\phi_0(z) = e^{i\eta_{\alpha_0}(z-z_0)} + Re^{-i\eta_{\alpha_0}(z-z_0)}, \qquad z < z_0, \tag{6}$$

where

$$\eta_{\alpha_0} = k_{\alpha_0}\cos\theta,$$

$$R = \text{unknown reflection coefficient}, \tag{7}$$

$$\phi_n(z) = a^+e^{i\eta_{\alpha_n}(z-z_{n-1})} + a^-e^{-i\eta_{\alpha_n}(z-z_{n-1})}$$
$$\psi_n(z) = b^+e^{i\eta_{\beta_n}(z-z_{n-1})} + b^-e^{-i\eta_{\beta_n}(z-z_{n-1})}, \quad z_{n-1} < z < z_n$$

$$n = 1, 2, \cdots, N-1.$$

If the laminate is totally immersed, i.e., the lower medium is fluid,

$$\phi_N = a_N e^{i\eta_{\alpha_N}(z-z_{N-1})}, \qquad z > z_{N-1}. \tag{8}$$

If the lower medium is air,

$$P(z_{N-1}) = 0 \tag{9}$$
$$T(z_{N-1}) = 0.$$

In matrix format, the stress-displacement vector $\{S(z)\}$ is defined as

$$\{S(z)\} = [U(z), W(z), P(z), T(z)]^T. \tag{10}$$

15

For perfect bonding between layers it can be shown that

$$\{S(z_n)\} = [A(n)]\{S(z_{n-1})\}, \tag{11}$$

where $[A(n)]$ is the so called "layer matrix" for the nth layer. Successive use of Equation (11) gives

$$\{S(z_{N-1})\} = [J]\{S(z_o)\}, \tag{12}$$

where $[J]$ is the 4 x 4 product

$$[J] = [A(N-1)][A(N-2)] \cdots [A(1)]. \tag{13}$$

Equation (12) relates the stress-displacement vectors at the top and bottom of the multilayered plate, with or without the presence of fluid. From Equations (6) and (8),

$$\{S(z_o)\} = [U_o \quad i\eta_{a_o}(1-R) \quad -\rho_o\omega^2(1+R) \quad 0]^T, \text{ and}$$

$$\{S(z_{N-1})\} = [U_N \quad i\eta_{a_N} a_N \quad -\rho_N\omega^2 a_N \quad 0]^T. \tag{14}$$

Equation (12) now gives a system of four linear equations for the four unknowns, U_o, R, U_N, a_N. In particular they can be solved to give R.

$$R = \frac{K_{3142} + q'q\, K_{2143} + i(qK_{3143} + q'K_{4122})}{K_{3142} - q'q\, K_{2143} - i(qK_{3143} - q'K_{4122})}, \tag{15}$$

where

$$q = \rho_o\omega^2/\eta_{a_o}, \qquad q' = \rho_N\omega^2/\eta_{a_N}, \tag{16}$$

and the indexed quantities are related to the elements of J through equations of the form:

$$K_{ijkl} = J_{ij}\, J_{kl} - J_{il}\, J_{kj}. \tag{17}$$

16

If the fluids at top and bottom are identical, then q=q'. In the absence of fluid at the bottom, q'=0. Equation (15) gives the desired reflection coefficient for a multilayered plate with fluid on one or both of its faces.

The Lamb wave dispersion equation is given by

$$K_{3142} = J_{31}J_{42} - J_{32}J_{41} = 0. \tag{18}$$

This equation was solved to yield Lamb wave phase velocity as a function of frequency. Calculated results for a three-layered laminate of 1 mm total thickness are shown in Figure 5.

Values of $R(\theta,\omega)$ were computed using Equation (15). The results for a uniform metal plate, 1.55 mm thick, with water on both faces, insonified at an angle of 15 deg to the normal, are shown in Figure 6. Figure 7 shows analogous results for a rubber backed steel plate with water on both faces. A three-axis plot of |R| versus frequency and angle of incidence for a similar steel/rubber laminate immersed in water is shown in Figure 8. The traces associated with symmetric Lamb waves and those associated with antisymmetric Lamb waves are identified in the figure.

It should be noted that the theory discussed above can be extended to anisotropic as well as dissipative media with full or partial debonding between the laminae.

4.0 EXPERIMENTS

This section describes the measurements that were performed at TRI and DAC to demonstrate the feasibility of employing the LLW method to detect and delineate debonds in metal/rubber laminates. Section 4.1 is a brief description of the TRI instrumentation. The DAC instrumentation is generically similar but

17

Figure 5

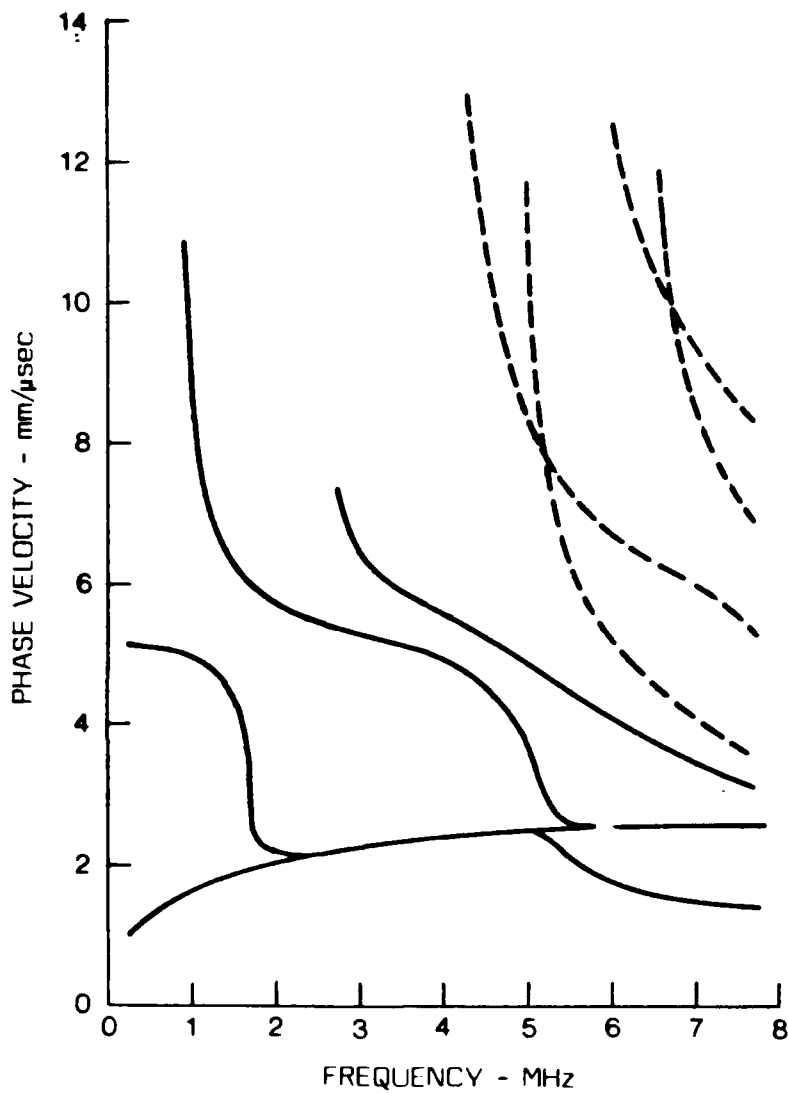Calculated dispersion curves for a 3-layer plate.
(After Mal [14].)
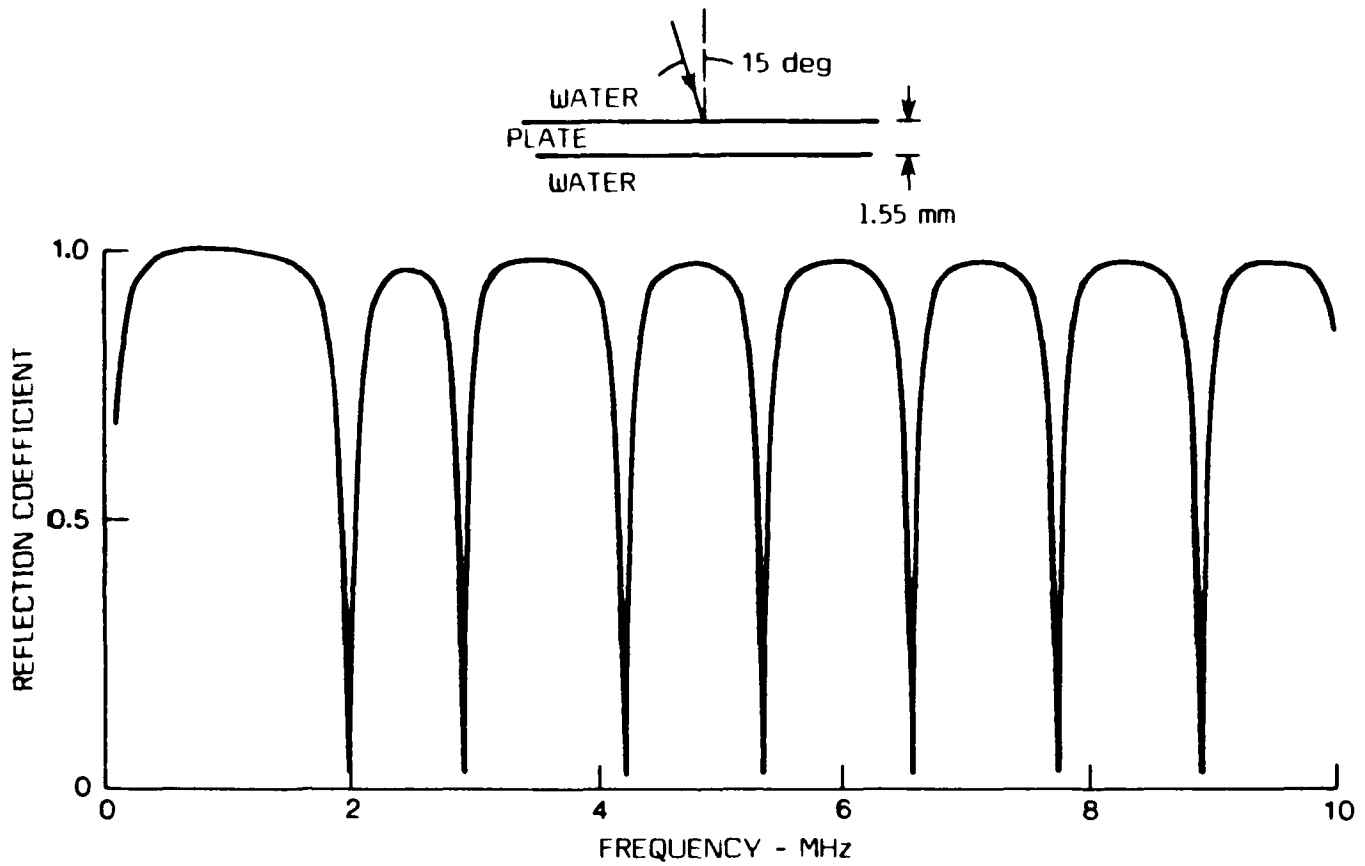
Figure 6

Calculated reflection coefficients for a 1.55 mm thick metal plate
immersed in water.
(After Mal [14], Equation 15.)
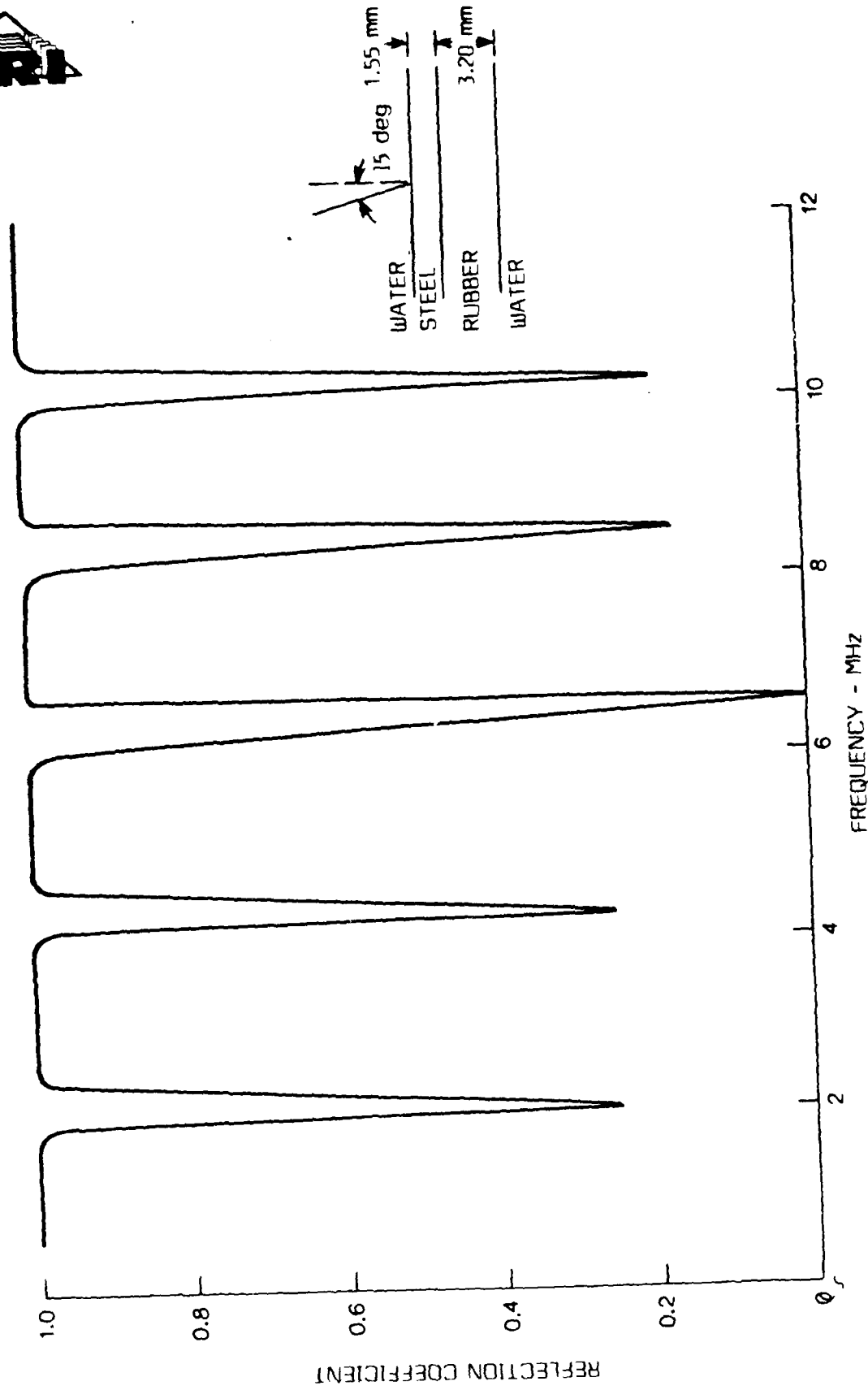
Figure 7

Calculated reflection coefficients for a 1.55 mm thick metal plate
backed by a 3.20 mm thick rubber layer, the whole laminate
immersed in water.
(After Mal [14], Equation 15.)

Insonification angle: 15 deg

Figure 8

Three-axis display of calculated reflection coefficients for a
steel/rubber laminate immersed in water. The tracks labelled "S" are
for symmetric waves, those labelled "A" are for antisymmetric waves.

includes computer control and color-enhanced C-scan capability. Section 4.2 is a discussion of specimen preparation; specific specimens are described in conjunction with the results of their ev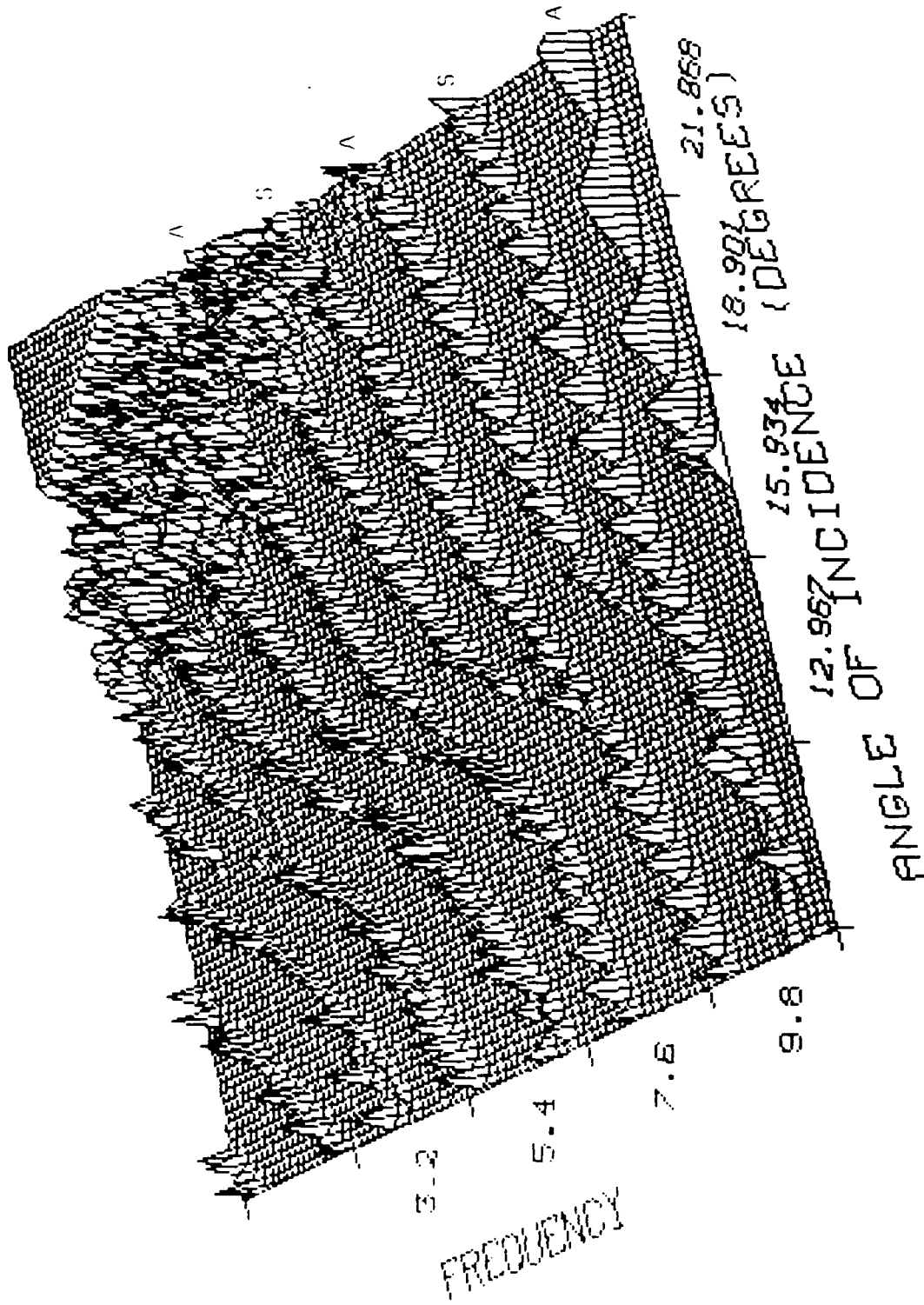aluation. Included in Section 4.2 is a brief description of the TRI method for preparing a partially bonded interfacial surface. Section 4.3 describes the set-up and measurement procedures employed at TRI and Section 4.4 presents the measurement results. Section 4.5 describes a new, quantitative method for evaluating the degree of adhesion between the rubber and metal adherends and includes some preliminary results of the application of the method to one of the specimens examined.

4.1 Instrumentation

Figure 9 is a block diagram of the experimental set-up. Figure 10 is a detailed drawing of the transducer mount. A photograph of the transducer mount and specimen support block is shown in Figure 11.

Bar-Cohen's work had indicated an optimal frequency range of 1 to 10 MHz for Lamb wave excitation. The transducers used in the present work were resonant at 4.4 MHz with a half-amplitude bandwidth of 3.8 MHz (2.5 to 6.3 MHz). The DP2020 Polynomial Waveform Synthesizer was programmed to generate either a linear frequency-modulated tone burst (LFM chirp) from 3.5 to 7.0 MHz or a single-frequency tone burst (truncated sinusoid) at a Lamb mode frequency near the resonance frequency of the transducer. Signal duration in either case was 8 μsec, or about 40-50 cycles of the sinusoidal signal. The LFM chirp was used during system initialization for detection of Lamb wave excitation and for evaluation of the modal frequencies (see Section 4.3). A single-frequency tone burst was used during specimen assessment, i.e., during scanning of a bond surface (see Sections 4.3 and 4.4).

The DP2020 drove the transmitting transducer through an ENI 240L RF Power Amplifier (20 MHz bandwidth). Drive level was set to yield maximum undistorted

22

Figure 9

Diagram of experimental set-up

SUPPORT AXIS

ACOUSTIC AXIS

TRANSDUCER
(Transmitter)

TRANSDUCER
(Receiver)

TRANSDUCER SUPPORT
BLOCK

15°

4.76 cm
(1.87 in.)

7.1 cm (nom.)
(2.8 in.)

1.1 cm (nom.)
(0.4 in.)

WATER

STEEL PLATE

RUBBER LAYER
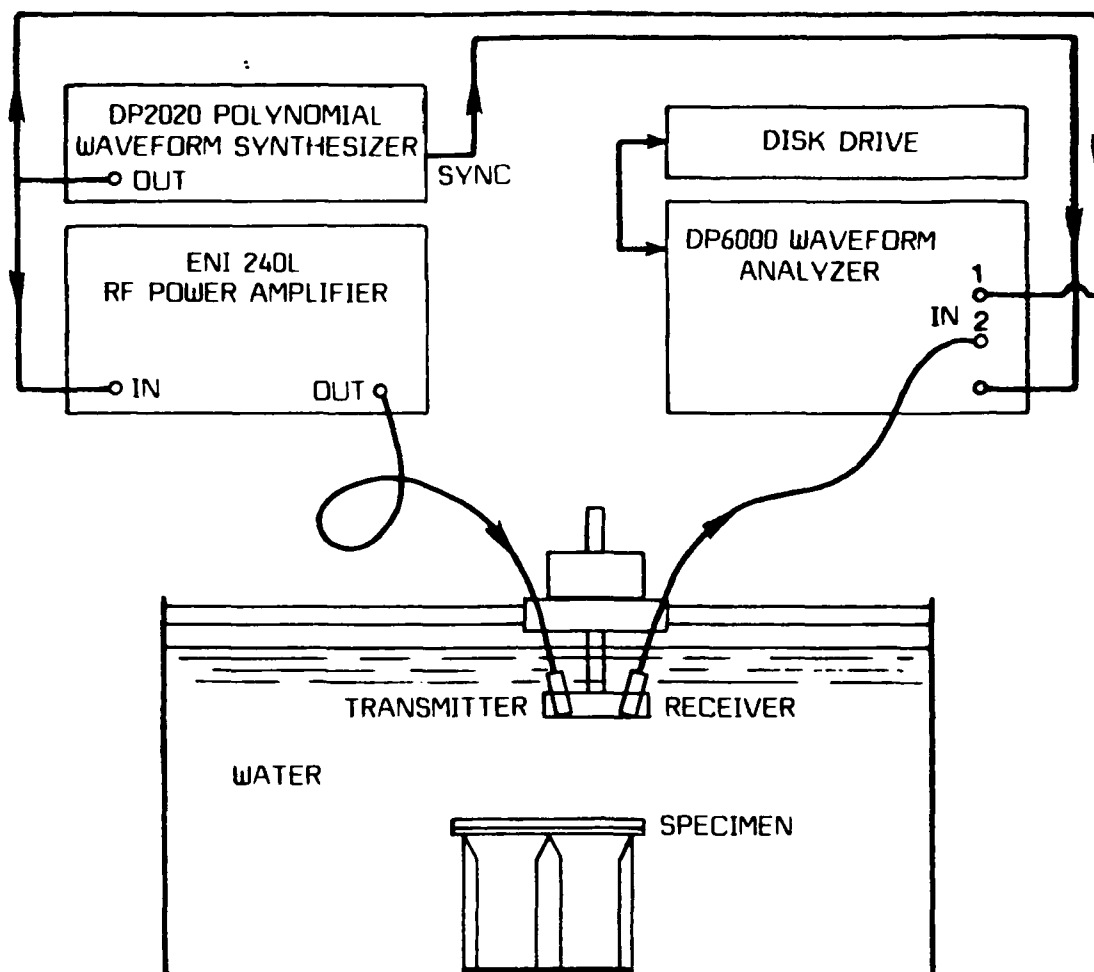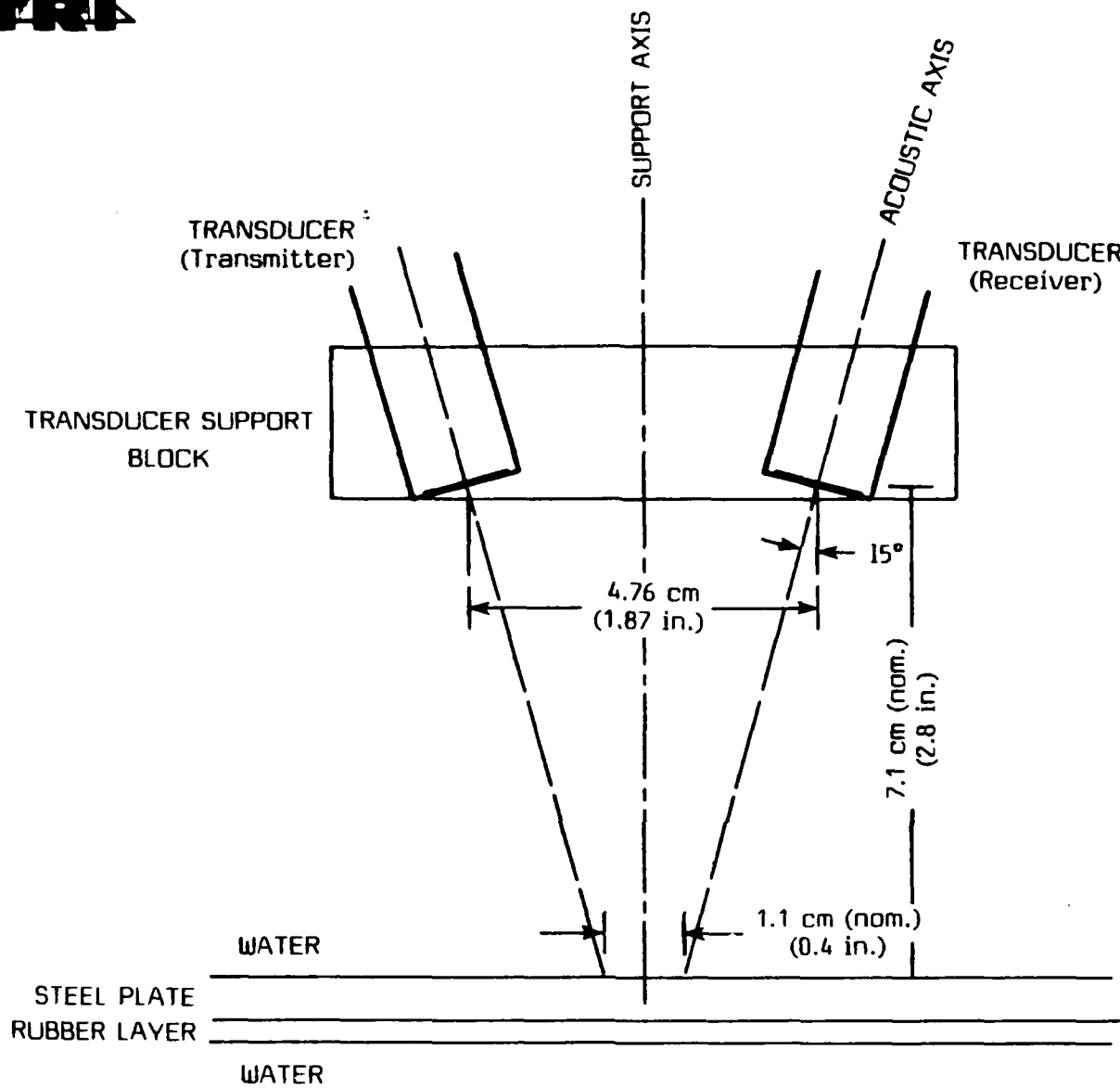
WATER

Figure 10

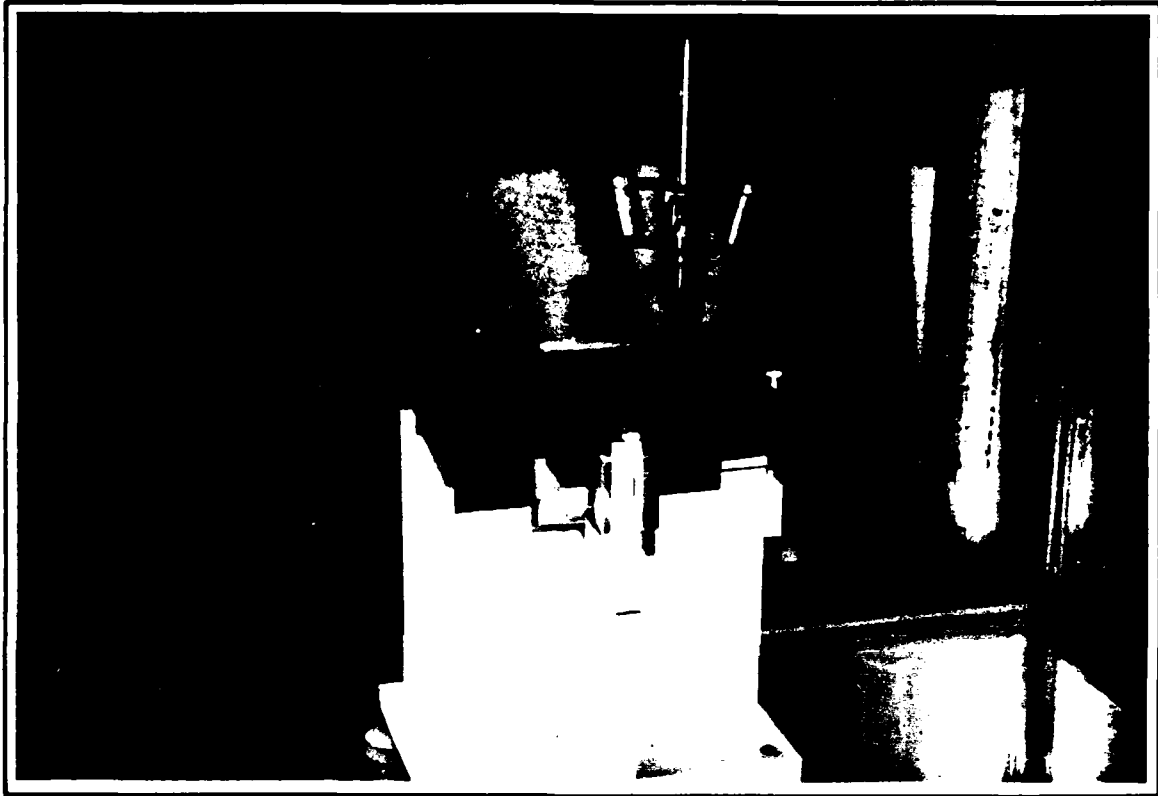Transducer arrangement for LLW measurements.

Figure 11

Photograph of transducer and specimen support apparatus.

acoustic signal level at the output of the receiving transducer. The signal
repetition rate was set at maximum permissible rate without interference from
overlapping "multipath" signals in the immersion tank.

Early measurements were made using independent, adjustable transducer
positioners. A range of incidence angles and transducer separation distances
(which determine transducer lift-off distance, the vertical distance from the
transducer face to the surface of the specimen) was investigated to determine
the transducer mount configuration shown in Figure 10. Subsequent use of a
single, fixed, two-transducer mount facilitated the ease and reliability of
measurement (scanning).

The received acoustic signals (FM or single-frequency) were input directly
to the DP6000 Waveform Analyzer. The waveform analyzer was used to make time
and amplitude measurements on the signals, perform time/frequency transforms and
cross-correlations, and evaluate and track the signal measurement parameter (RMS
level) during scanning. Specific applications of the DP6000 are described in
Sections 4.3 and 4.4. Signal waveforms and signal analysis results, i.e.,
Fourier spectra, correlation functions, etc., and surface scan data were stored
on magnetic disk for subsequent processing and plotting in hard copy using an
external system.

4.2 Specimens

Several planar, bonded rubber/metal specimens were prepared and tested.
The metal used was Type 304 cold-rolled stainless steel with thicknesses of
0.16, 0.32 and 0.64 cm (0.06, 0.12 and 0.25 in.). Stainless steel was selected
to avoid corrosion (rusting) during prolonged periods of water immersion.
However, cold-rolled stainless steel is anisotropic and inhomogeneous, affecting
wave propagation in the material. Efforts to resolve some of the problems

caused by property variations led to several innovative and beneficial techniques for setting-up and/or making measurements and for processing the signals or scans to improve detection and discrimination of bond surface flaws.

Neoprene 5109S was bonded to the metal adherends according to the following procedure. The metal plate was vapor degreased in trichloroethane for 30 min, then grit-blasted with No. 50 coarse steel grit. The grit-blasted surface was then wiped with methylethylketone and vapor degreased again for 30 min. Two coats of Chemlok 205 primer were applied, allowing 30 min minimum drying time per coat. This was followed by application of two coats of Chemlok 220 adhesive, again with 30 min minimum drying time per coat. The neoprene was then vulcanized to the prepared plate at a temperature of 157°C (315°F) for 55 min at 138×10^3 kPa (20 ksi) pressure.

At the time this Phase I work was proposed there was uncertainty regarding the thickness-to-wavelength limit for exciting Lamb waves in a metal/rubber laminate. It was known from Bar-Cohen's work that Lamb waves could be excited in thin plates 0.16 cm (0.06 in.) thick (thickness-to-wavelength ratio about 1.0). Specimens were thus prepared initially from 0.16 and 0.32 cm (0.06 and 0.12 in.) material to establish and confirm set-up and measurement procedures. A focus of several NDE efforts at TRI has been and continues to be the head-mass assembly (HMA) of the TR-317( ). The adherend thicknesses in this structure are about 0.64 cm (0.25 in.) thick metal and 0.32 cm (0.12 in.) thick rubber. Therefore, after it was demonstrated that Lamb waves could be excited in a specimen of these dimensions and could be successfully used to detect and delineate flaws in the bond surface, little further attention was given to the thinner materials. That is, the results reported in the following section are, for the most part, for 0.64 cm (0.25 in.) thick metal plates bonded to 0.32 cm (0.12 in.) thick rubber.

TRI developed a quantifiable way to prepare a less than fully bonded surface. The basis of the method is to mask the metal surface with a screen prior to application of adhesive. The screen allows adhesive coverage of a specifiable fraction of the surface area. An example is shown in Figure 12. This figure shows the adhesive surface of a 0.64 cm (0.25 in.) thick plate prior to bonding the rubber layer. The left half of the surface has 100% adhesive coverage; the right half has 75% adhesive coverage as determined by the ratio of the bare metal circles to the total area of the half-surface. More or less coverage is achieved by using different sized and/or different numbers of circles in the masking screen. It is important that the circle size be small enough that the area being interrogated by the acoustic beam includes, on average, covered (adhesive) and exposed (no adhesive) portions in the ratio specified for the total surface area.

Simple debonds--strip debonds running from edge-to-edge across the specimen, or spot debonds at random locations in the bond surface--were programmed by masking the prepared metal surface prior to application of the Chemlok 205/220 adhesive system. The masking strip or spot was removed before vulcanizing the rubber layer.

Specific specimens are detailed in the discussion of results in Section 4.4 below.

4.3 Set-Up and Recording Procedures

The Lamb mode frequencies (within the bandwidth of the ultrasonic system) were determined by insonifying the surface of a specimen with a broad-bandwidth signal at an oblique angle of incidence in the range from about 10 to 22 deg.
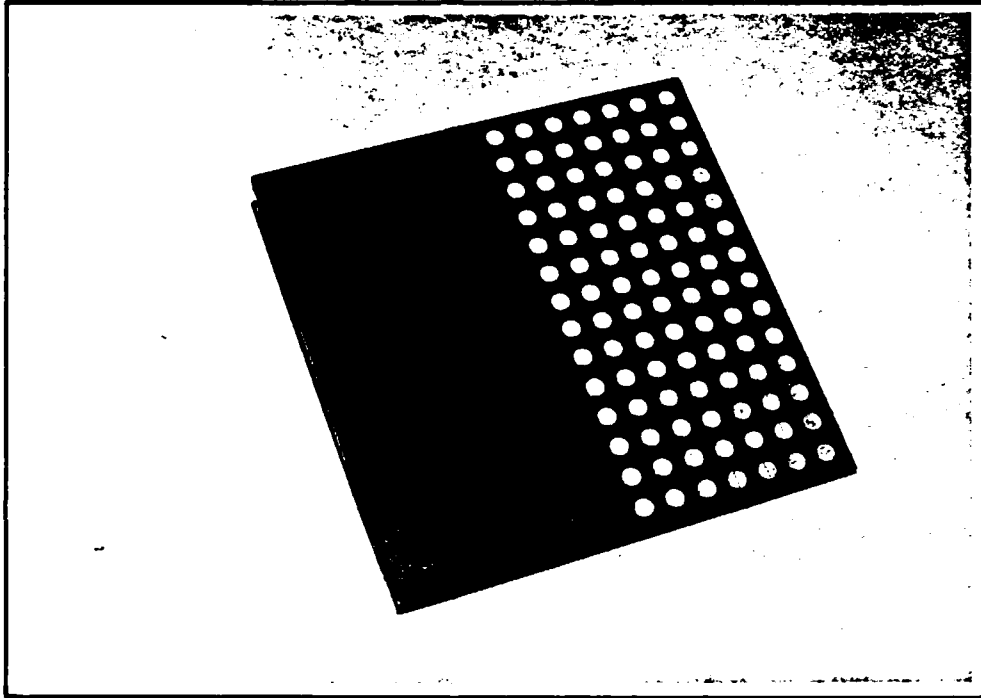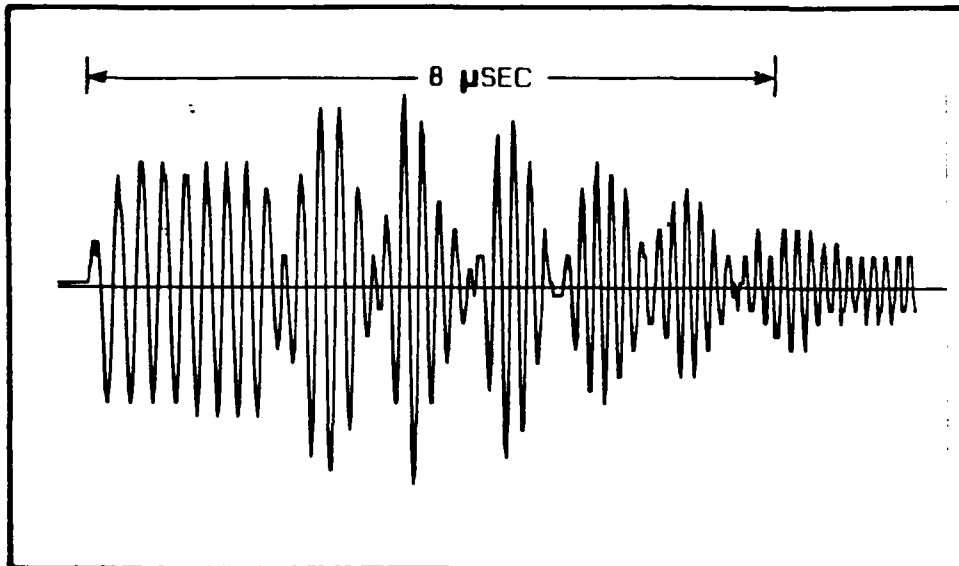
Figure 12

Photograph of the adhesive surface of a 15 cm (6 in.) square steel plate.
The left half of the plate has 100% adhesive coverage. The right half of
the plate had adhesive applied over masking disks in the pattern shown
to yield 75% areal coverage of adhesive. The disks were removed
after the adhesive had dried.

Both an impulse-like signal and a frequency modulated tone burst (FM chirp) were used. If an impulse-like signal was used, the procedure was to compute the Fourier spectrum of the received signal and observe its character as the receiving transducer was moved across the reflected/reradiated interference sound field. Lamb wave excitation resulted in the appearance of numerous spectral nulls at the Lamb mode frequencies. If a FM chirp was used, the procedure was to first scan the receiving transducer across the reflected/reradiated sound field until an interference pattern was observed in the received signal, then compute the Fourier spectrum of this signal. The spectrum exhibited numerous nulls at frequencies corresponding to those of the Lamb wave modes. TRI used a FM chirp as an insonifying signal; DAC used an impulse-like signal.

Figure 13(a) shows a typical interference waveform for a 0.64 cm (0.25 in.) thick plate insonified with a 3.5 to 7 MHz FM chirp. Once detected, an interference waveform was maximized by adjusting the lift-off of the transducers to obtain a strong null structure. The Fourier spectrum of the waveform was then computed. Figure 13(b) shows the Fourier spectrum (FFT) of the waveform illustrated in Figure 13(a). The nulls in this spectrum reveal the frequencies of the Lamb wave modes that were excited. (Note that this discussion assumes a fixed geometry. If the geometry is changed, a different distribution of modes, i.e., spectral nulls, will be observed.)

LLW modal excitation is less sensitive to transducer alignment at insonification angles less than about 20 deg to the surface normal. DAC performed preliminary scans across one of the specimens at insonification angles of 13, 15, 17, 19 and 21 deg and concluded that the maximum signal difference between bonded and debonded surfaces occurred at 15 deg. This angle was subsequently used for all measurements.

(a) INTERFERENCE NULL SIGNAL WAVEFORM
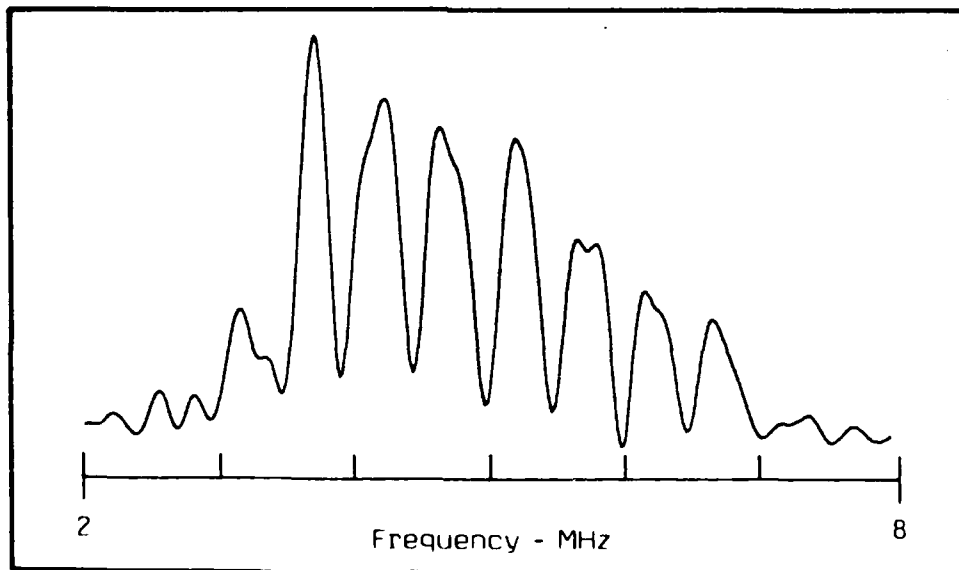
(b) FOURIER SPECTRUM OF
INTERFERENCE NULL SIGNAL WAVEFORM

Figure 13

Broad-bandwidth FM chirp interference null waveform and its Fourier spectrum.
The specimen was a 0.64 cm (0.25 in.) thick steel plate. The Lamb wave mode frequencies
are identified by the frequencies at the nulls of the spectrum.

The next step in setting-up was to choose a modal frequency for use in specimen evaluation. There is presently no a priori basis for selecting one modal frequency in preference to another. The procedure employed was to pick the modal frequency closest to the resonant frequency of the transducers to maximize acoustic signal level, or the next higher or lower modal frequency if one of these displayed a deeper spectral null. The specimen was then insonified with a tone burst signal at that modal frequency. This resulted in a null signal waveform at the receiver like that illustrated in Figure 14. The initial high-level portion of this signal is that part of the specularly reflected incident wave received before the interfering reradiated Lamb wave reaches the receiver. The comparable high-level portion at the end of the signal is that part of the reradiated Lamb wave remaining after the interfering specularly reflected incident wave has terminated. The low-level region in between these relatively high-level portions of the overall signal is the null signal resulting from the destructive interference between the specularly reflected and reradiated waves. The measurement window indicated in the figure was positioned within the null region of the signal as illustrated.

Figure 14 was recorded over a well-bonded area of a bonded metal/rubber specimen. Debonding will change the acoustic characteristics of the bond surface; this will change the Lamb mode structure in the region where the debonding occurs. Reflectivity and refractivity will be altered changing the path length, i.e., relative phase, and amplitude of the leaky Lamb wave along the axis of interference with the reflected wave. Consequently, the null signal will be degraded, i.e., the depth of the null will be lessened. Operationally, an increase in signal amplitude will result from a change in the quality of the bond between the rubber and metal layers.
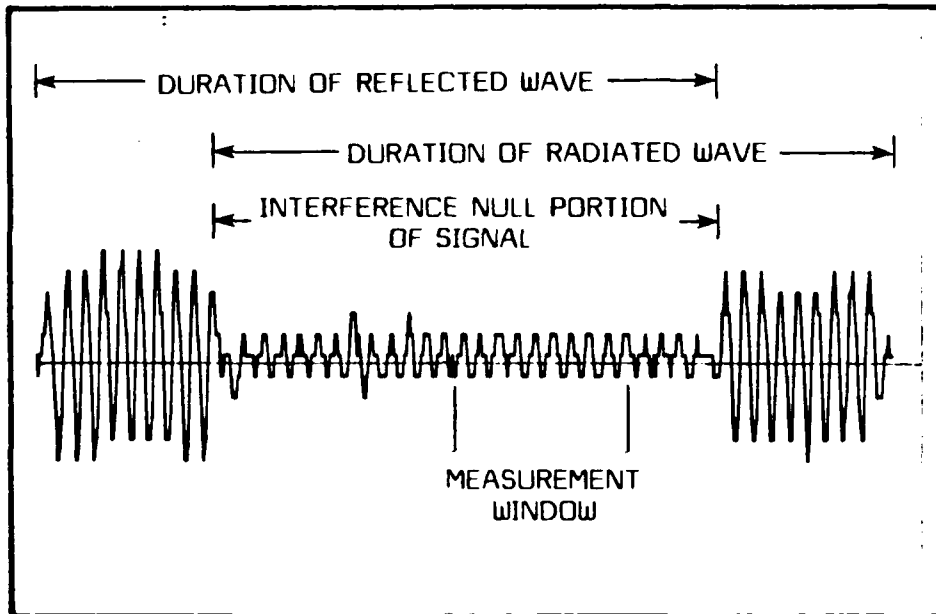
Figure 14

Interference null waveform generated by insonifying a metal/rubber laminate
with a narrow-bandwidth tone burst signal. The waveform was recorded over
a well-bonded area of the bond surface.

Although it was known prior to beginning this work that material anisotropy and/or inhomogeneity could degrade the sensitivity and reliability of the measurements, the sometimes large effects actually experienced were unexpected. Until the magnitude of the effects was recognized (relatively late in the program), set-up, or system initialization, and scanning were routinely done with the plane containing the transducers oriented normal to the direction of scanning. This provided maximum edge-to-edge surface coverage during a scan.

A single measurement comprised the average signal level within the null signal window (see Figure 14) after a single transmission. TRI computed the average RMS value; DAC used the average of the rectified gated waveform. A scan line was generated by tracking sequential measurements as the transducers were moved across the specimen. Following selection of a modal operating frequency and generation of a tone burst signal at that frequency, the transducer lift-off distance (see Section 4.1) over the initialization site was adjusted by observing the averaged signal level while moving the transducers toward and away from the surface of the specimen. The lift-off distance was fixed at the position which yielded the lowest average level, which, if the initialization site was a well-bonded area, constituted the lowest background signal level.

Once the effects of material anisotropy and inhomogeneity (e.g., grain scattering) on signal-to-background ratio were recognized, further adjustment to reduce background signal level was made by rotating the transducers about their support axis (see Figure 10) to align the transducer plane with, for example, the orientation direction of the material grains, or whatever other anisotropy was present. This minimized signal loss due to scattering or refraction.

34

The preceding steps--selection of an operating frequency and the adjustments to minimize the background level--constituted system initialization. After the system was initialized, the specimen was scanned.

Specimens were scanned line-by-line, with a single measurement every 0.13 to 0.16 cm (0.05 to 0.06 in.) in the direction of transducer motion. As noted above, a scan line was generated by tracking the sequential measurements as the transducers moved across the surface. Following generation of a line, the transducers were moved laterally, i.e., perpendicular to the scanning direction to generate a new scan line. The C-scan results shown in the following subsection were obtained with a scan line separation of 0.02 cm (0.01 in.).

C-scan images were generated as follows. The signal (averaged, windowed interference null waveform) was input to a TEK 6230 Intelligent Graphics Work-station. The dynamic range of the signal and the number of signal level bins within this range were selected by the operator. Signals within each bin were represented by a particular color on the Workstation CRT. The TEK 6230 also monitored the position of the transducer pair relative to the bond surface being scanned. A color-enhanced C-scan image of the bond surface was generated as the amplitude level of the interference null signal drove the color of the cursor of the CRT of the TEK 6230, which tracked the position of the transducers. That is, each pixel on the CRT display represented a data acquisition point on the bond surface of the specimen. Signal levels and transducer position coordinates were stored for subsequent off-line preparation of color-coded hard-copy plots (C-scan images).

4.4 Results

As stated earlier, the primary goal of this Phase I effort was to demonstrate the feasibility of using the leaky Lamb wave method to detect flaws in bonded metal/rubber laminates. A secondary goal was to examine application of the method to evaluation of bond quality (surface adhesion) through implementation of a new, quantifiable method to prepare a partially bonded surface. Results are presented in this section to show that these goals were achieved.

Figure 15 is a diagram of a 0.64 cm (0.25 in.) thick steel, 0.32 cm (0.12 in.) thick rubber specimen prepared with a strip debond at the steel/adhesive interface. The grit-blasted surface of the steel plate was masked with a 1.27 cm (0.50 in.) wide strip of Teflon® tape prior to application of the Chemlok 205/220 adhesive system. The Teflon® strip was removed to expose the bare metal surface before bonding the rubber to the plate. After this specimen was prepared, the strip debond was opened to a depth of about 3.8 cm (1.5 in.) at each end by forcibly inserting and removing a 0.02 cm (0.01 in.) thick spatula. The center portion of the strip was left intact. After removal of the spatula, the rubber and metal adherends returned to a state of touching.

Figure 16 is a scan line recorded about 2 cm (0.8 in.) inboard of the lower edge of the specimen shown in Figure 15, i.e., across the mid-part of the lower "opened" portion of the debond strip. The insonifying signal frequency was 4.13 MHz. The bond flaw signature is readily apparent in this scan line. The signal-to-background ratio, measured as indicated in the figure, is 3.5 dB. Note the apparent horizontal offset of the signal from the true location of the debond. This occurs because the signal level begins to rise when the sound beam first enters the debond area and begins to fall when the beam begins to exit the area.
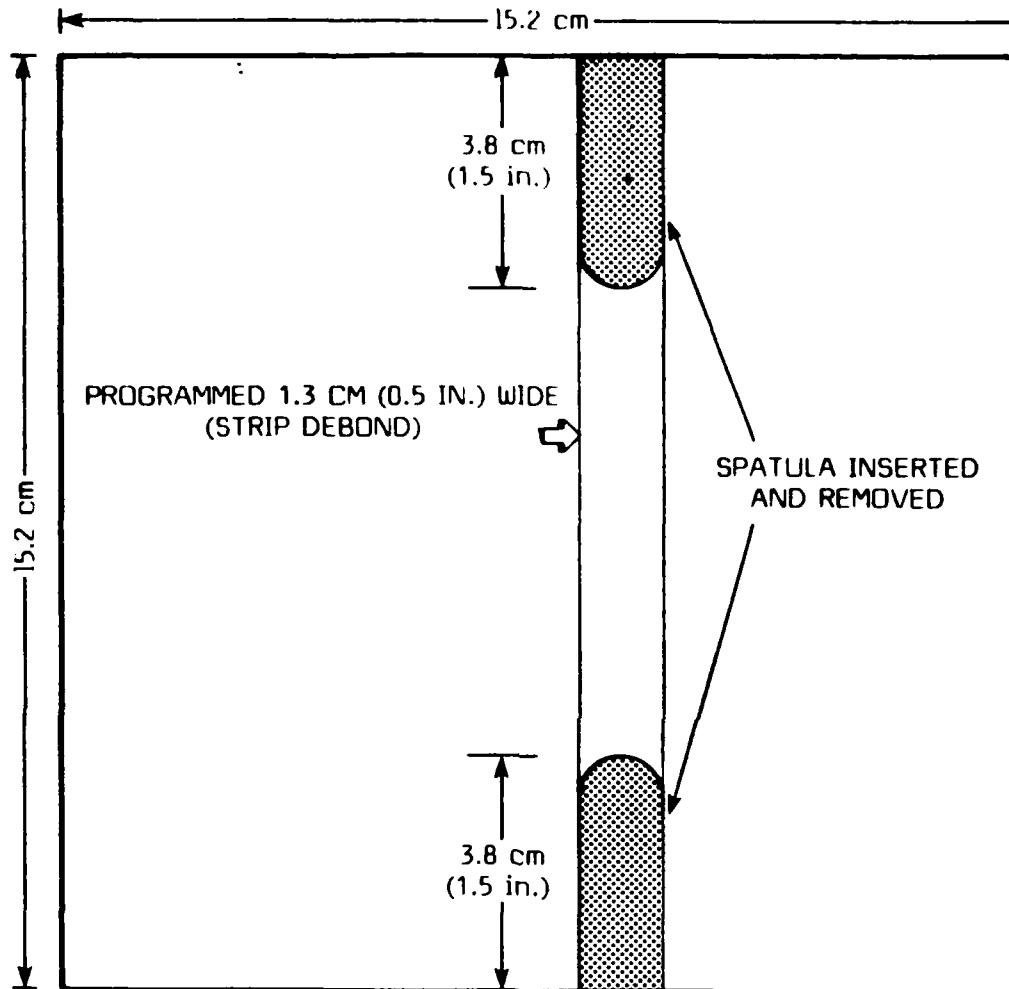
Figure 15

Sketch of bond surface of a 15 cm (6 in.) square metal/rubber specimen with a programmed strip debond.
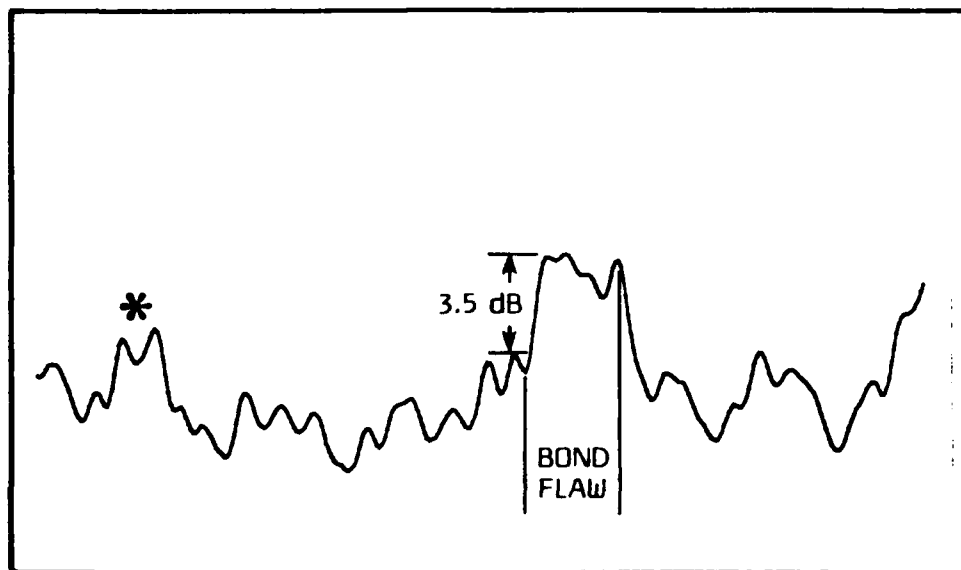
Figure 16

Single scan line across the strip debond specimen. The specimen
is diagrammed in Figure 15. The "flaw signature" marked by the asterisk does not
appear consistently at other insonifying frequencies (see text).

A second, flaw-like signature, marked by the asterisk, appears at the left end of the scan line in Figure 16. Analogous scans along the same line across the specimen made at the next three higher modal frequencies indicate that this apparent flaw is a frequency dependent perturbation in the background signal level. These scan lines, at 4.46, 5.15 and 5.65 MHz, together with the line from Figure 16, are shown in Figure 17. All four lines are indexed to the known flaw signal. The questionable flaw-like signature either does not appear in the other frequency lines or it does not repeat at the same location indicating it apparently is not related to any change at the bond interface.

If, as indicated in Figure 17, there is a differential sensitivity to frequency between flaw (signal) and adherend (background), then summing or averaging of lines recorded at several frequencies should improve the signal-to-background ratio much as these processing operations do for signal-in-noise. Indeed, this is the case for the scan lines shown in Figure 17. The sum of these four lines is shown in Figure 18. The signal-to-background ratio at the location of the bond flaw has increased 1.9 dB to 5.4 dB. (However, the ratio is 0.5 dB less referred to the background signal level in the region of the spurious flaw-like signature.)

Color enhanced C-scan images of this specimen using conventional pulse-echo and LLW methods were obtained by Bar-Cohen at DAC. Figure 19 shows two color enhanced C-scans of the strip debond specimen sketched in Figure 15. The scan on the left side of the figure was obtained using a conventional pulse-echo method; the scan on the right side, by the LLW method. The color range scales for the two images differ somewhat, so the signal-to-background ratio between a high-level signal spot within the debond strip and a nearby low-level background spot is given above each image. The location of the debond strip as indicated by the C-scan, i.e., not the true location (see Figure 16), is delineated by the
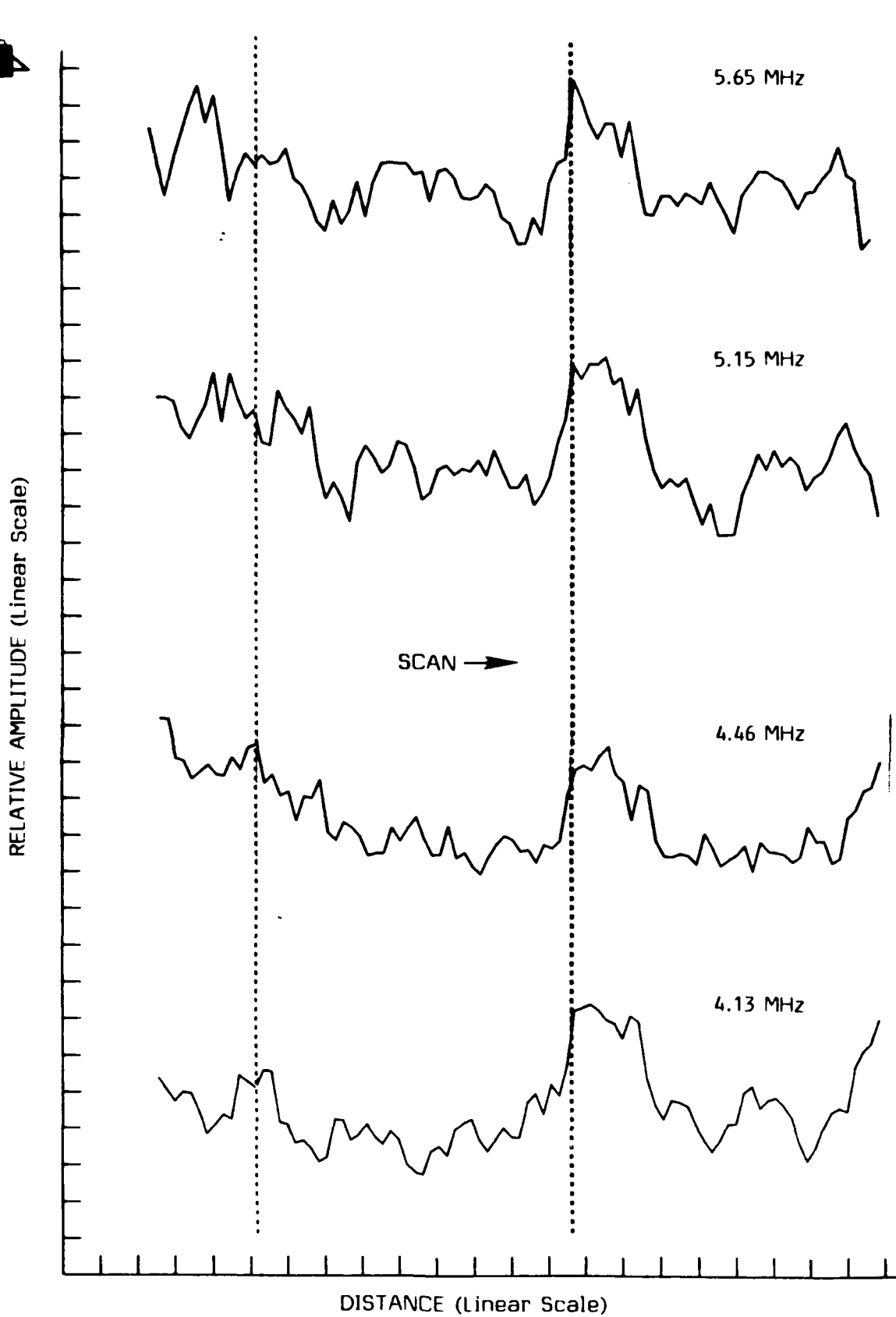
Figure 17

Single scan lines across the strip debond specimen at four adjacent
Lamb mode frequencies. The specimen is diagrammed in Figure 15.
The scan line at 4.13 MHz is repeated from Figure 16. The heavy
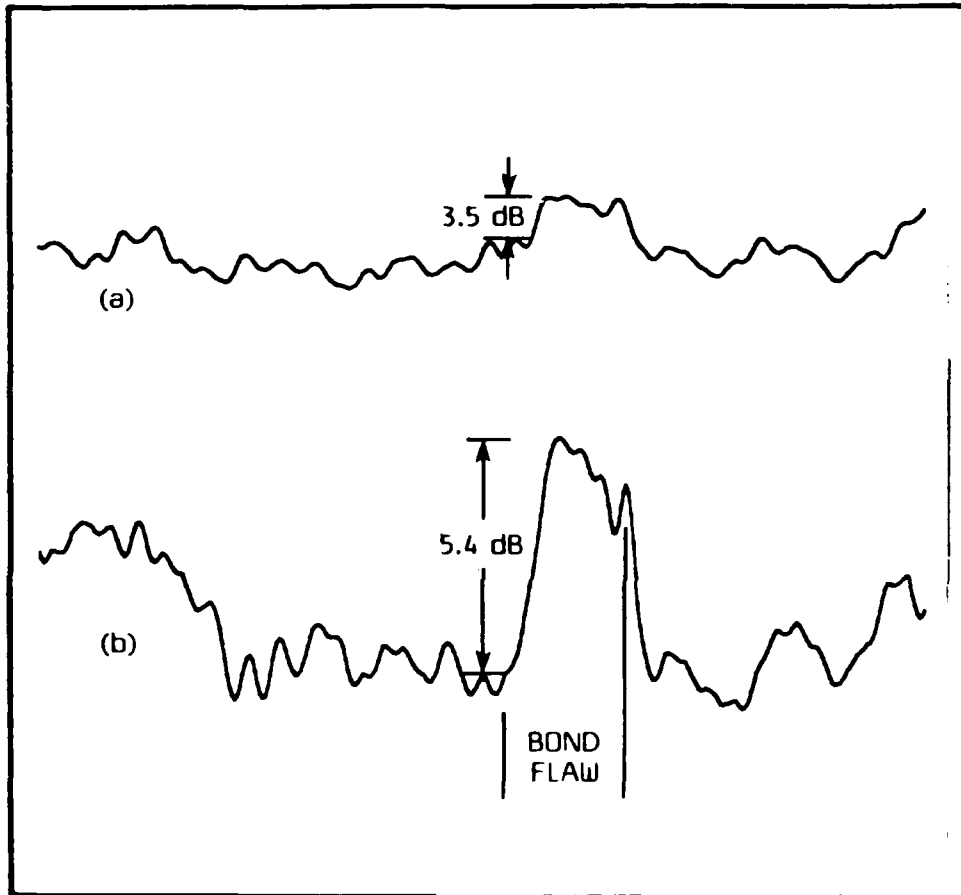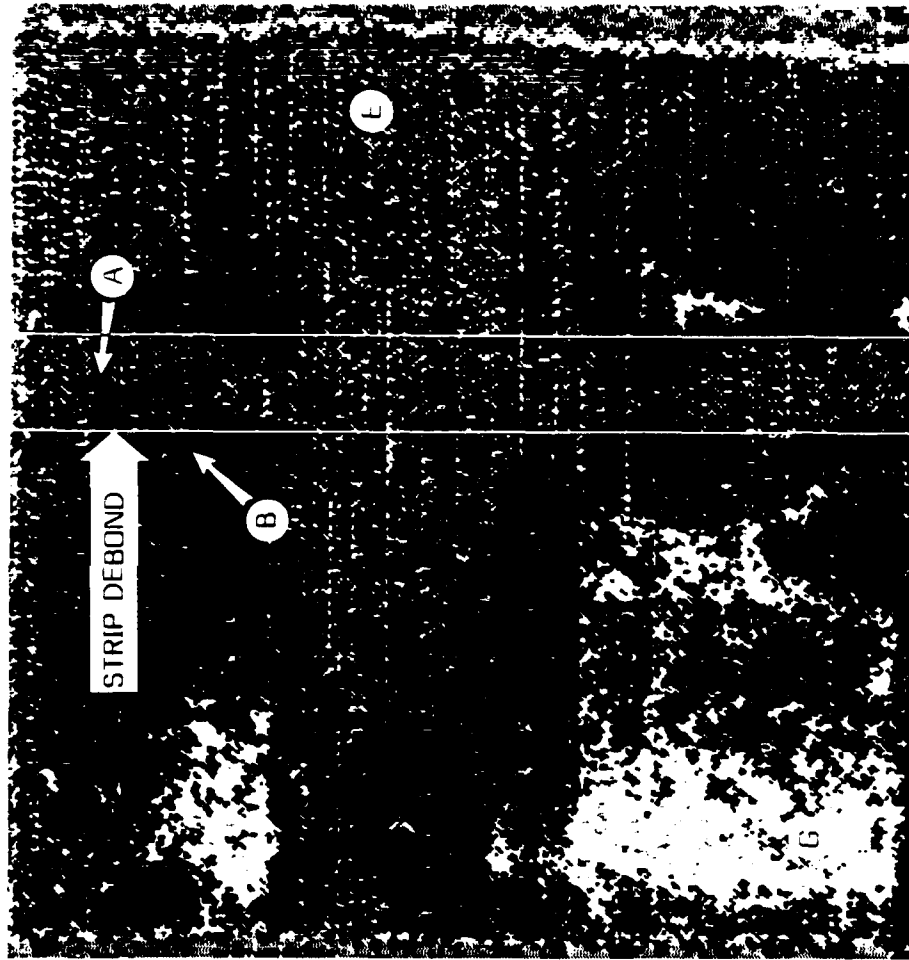broken line indexes the bond flaw signature.

Figure 18

Sum of single scan lines across the strip debond specimen
at four adjacent Lamb mode frequencies (see Figure 17).
The specimen is diagrammed in Figure 15.

(a) Single scan line at 4.13 MHz.
(b) Sum of scan lines.

(b) Leaky Lamb wave

A/B   6.3 dB
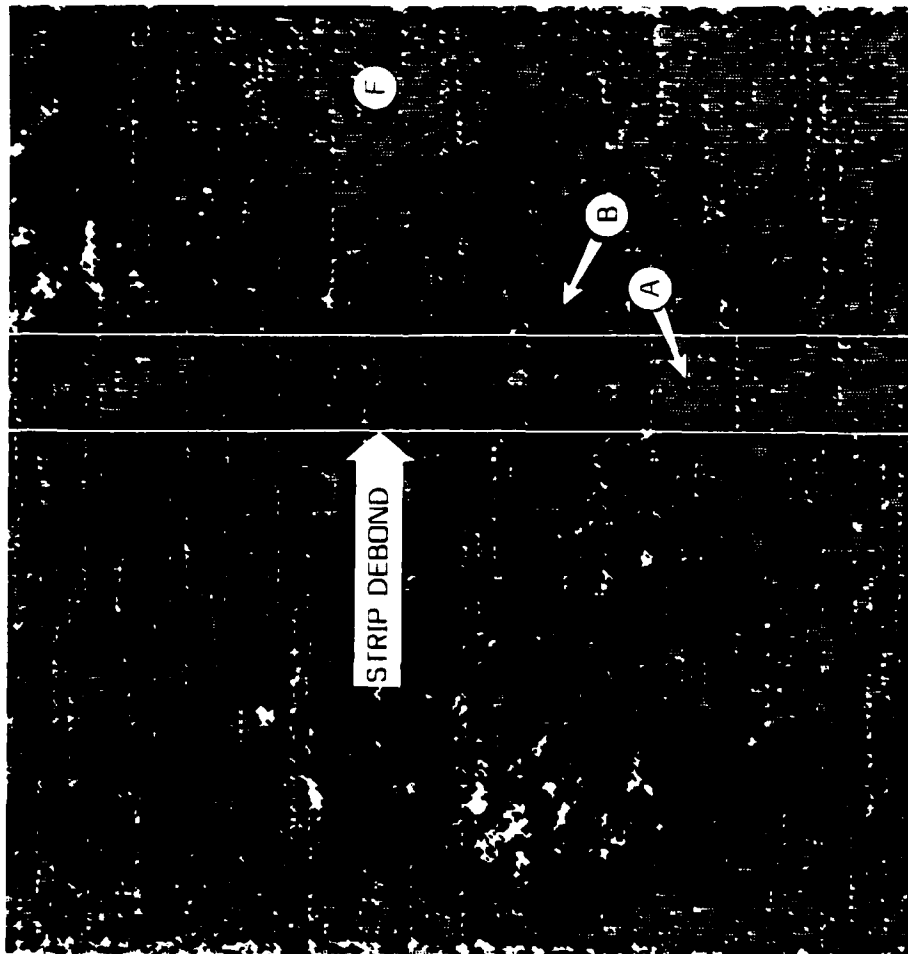
(a) Pulse-Echo

A/B   2.0 dB

Figure 19

Color enhanced C-scan images of the strip debond specimen. The specimen is diagrammed in Figure 15. (a) Image obtained using a conventional pulse-echo method. (b) Image obtained using the LLW method.

42

white vertical lines in each image. The actual location of the strip debond is slightly to the left of where the LLW image shows it.

The pulse-echo C-scan shows arguable detection of the debond strip at its lower end and one high-level spot at its upper end, with an appreciably lower overall signal-to-background ratio. The LLW method not only delineates the entire debond strip but images the various parts of it, i.e., the "opened" end portions and the unopened center portion. (The high-level signal area to the right of the debond strip in the LLW image, labelled E, is discussed in Section 4.5 below. The pulse-echo C-scan image also shows a comparable questionable area on the right, labelled F.)

A second generic class of bonding problem is that of poor bonds. That is, due to poor surface preparation, faulty adhesive, improper curing, or other cause, a structure with a homogeneous, but poorly bonded interface is fabricated. There are no debonds to detect or delineate. The task then is to evaluate the quality of the bond. The LLW method is eminently capable of performing this task, providing reliable reference specimens can be prepared.

TRI developed a method to prepare partially bonded surfaces with known percentages of adhesive coverage. This was described in Section 4.2 above. A typical scan line across the partially bonded specimen shown in Figure 12 is presented in Figure 20. The direction of the scan was from the 100% adhesive side to the 75% adhesive side. The insonifying frequency for this scan was 4.64 MHz. The plane containing the transducers (see Figure 10) was oriented at an angle of 15 deg to the scan direction, with the receiver leading, i.e., entering over each area first. The large peaks at the beginning and end of the scan line are edge effects caused by one or the other of the transducers' beams being
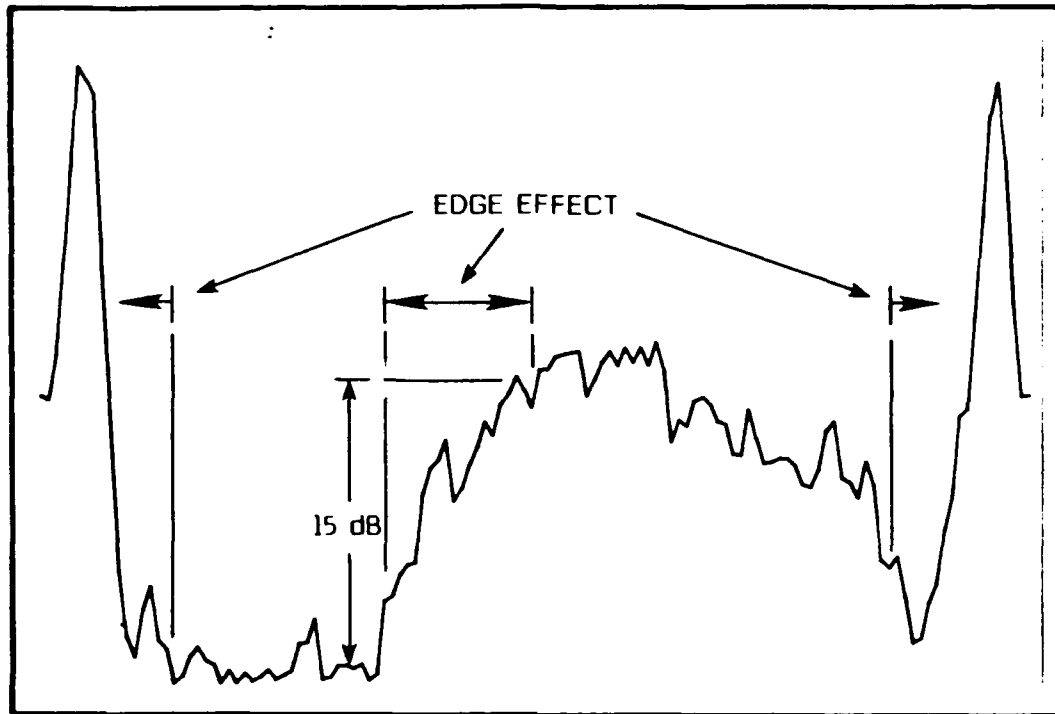
Figure 20

Single scan line across the 100%-75% adhesive coverage specimen.
The specimen is shown in Figure 12. The "edge effect" is caused by
the oblique orientation of the transducer plane to the
scanning direction.

44

partially on or off the plate. A similar effect occurs as the transducers move across the boundary delineating the two sides of the specimen, i.e., there is an increase in signal level as the transducers move from one bond surface onto the other.

When both transducer beams are on one or the other bond surfaces, the signal level is relatively constant. The change in average level from the fully bonded (100% adhesive coverage) to the partially bonded (75% adhesive coverage) surfaces in Figure 20 is about 15 dB. Thus, the LLW method is able to yield a measure of the bond quality given a known fully-bonded reference surface.
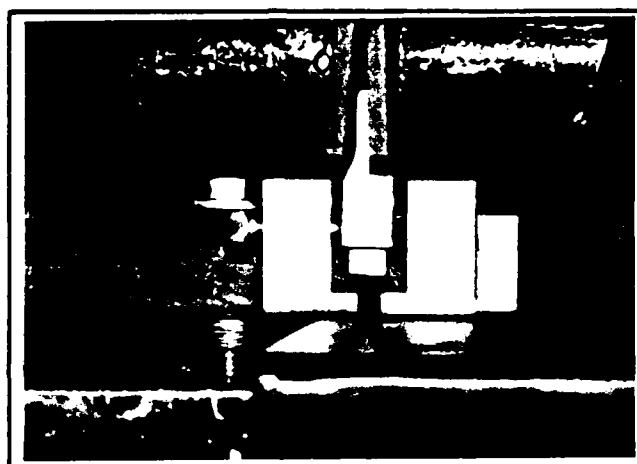
4.5 Rubber Pull Tests

The LLW C-scan image (See Figure 19(b)) of the strip debond specimen (see Figure 15) displays a high signal level region, E, to the right of the center and upper portions of the debond strip. With no additional information it could be concluded that this is a weakly bonded, or even debonded, area of the bond surface. In an attempt to unequivocally determine the bond state in this and other areas of the surface, destructive, controlled pull tests on the rubber layer were performed.

Standard test methods, e.g., a peel test, were deemed unsuited to the problem. Therefore, TRI devised a new method for evaluating bond state when the rubber adherend is thin. This method involves bonding a pull rod to a circular core cut in the rubber layer with a cyanoacrylate adhesive.
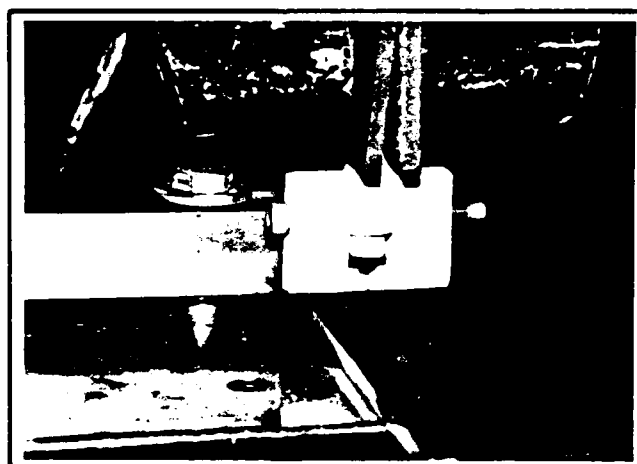
The actual pulling fixture is more complex than a simple rod as shown in Figure 21. The end of the rod has a boss which is inserted into a shallow cup cut into the rubber core surface. This increases the bonding area on the rod and provides added strength during the pull. The rod and metal/rubber specimen
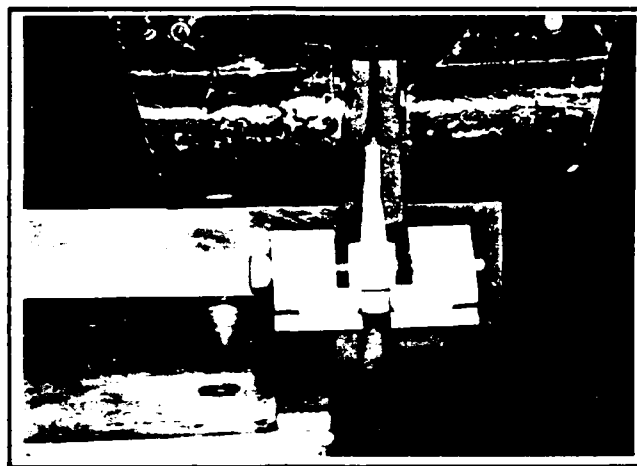
(a)

(b)

(c)

Figure 21

Photographs showing stages of a rubber pull test
(a) During initial pull. (b) Showing neck-down of rubber core; before
clamping arms on stretched core. (c) Showing fully clamped core
just before rubber separation (cohesive failure).

are fixtured in an Instron Universal Testing Machine. The rod is then pulled away from the specimen at a linear velocity of about 0.25 cm/min (0.10 in./min).

Pulling causes the rubber core to stretch and neck down along its length. Following sufficient stretch--about 0.5 cm (0.2 in.)--the L-shaped arms of the pulling fixture swing into alignment with the center rod and are then clamped about the center, necked-down portion of the stretched rubber core to provide added grip on the core piece. Pulling resumes until the rod/rubber bond surface separates or until the rubber core pulls away from the plate (adhesive failure), or, as was usually the case, the rubber fails (cohesive failure).

Several cores were pulled in the questionable area, E, of the specimen (see Figure 19(b)), in a presumably well-bonded area, labelled G in the figure, and in the center portion of the debond strip. Cores in the debond strip came out with the coring tool indicating no bonding occurred as programmed. Maximum pulling forces (resulting in cohesive failure) recorded for both of the other areas were 32 kg (70 lb), or 6.8 x 10^3 kPa (990 psi). That is, the questionable area appeared to be as well bonded as presumably well-bonded areas.

Therefore, other possible causes were sought for the high signal level in the questionable area. Careful examination of Figure 19(b) reveals that the area labelled E appears to be part of a wide "band" across the plate. The exact nature of this band is unknown, but it was assumed a posteriori from the LLW evaluation (Figure 19(b)) that the relatively high-level signal in this band was caused by some form of inhomogeneity or anisotropy in the steel plate. The background signal level in a scan can often be reduced by adjusting the orientation of the transducer plane relative to the scan direction. This minimizes signal losses due to scattering or other redirection of signal energy caused by inhomogeneity or anisotropy. In the present instance, a reduction in the overall signal level in the questionable area, E, of the apparent "band" was

47

noted, but the area did not completely disappear. Thus, it is presumed, but not confirmed, that the cause of the high signal level in the questionable area is a perturbation of unknown nature in the properties of the steel adherend. (It should be noted that the destructive pull tests performed on the present specimen preclude further acoustic evaluation of it.) The problem of signal loss due to anisotropy and/or inhomogeneity in the adherends is addressed in detail in the Phase II proposal to continue this work. It is a problem that will require much more examination than was possible during this Phase I effort.

5.0 CONCLUSIONS

On the basis of the work performed during Phase I it is concluded that:

- the feasibility of using the LLW method to detect and delineate bond flaws in metal/rubber laminates when the adherends remain in intimate contact was successfully demonstrated; the improved sensitivity of the LLW method over conventional pulse-echo ultrasonic methods was dramatically shown;

- the LLW method is capable of providing a quantifiable measure of the bond state, e.g., the degree of adhesive coverage, of a bond surface;

- variations in material properties, i.e., inhomogeneity, can deleteriously affect detection of a bond flaw or assessment of bond state, but there are straightforward procedural adjustments and/or signal processing measures which can reduce these effects.

6.0 RECOMMENDATIONS

This Phase I effort on NDE of adhesive bonds addressed and demonstrated the feasibility of using leaky Lamb waves to assess bond joints in metal/rubber

laminates. Based on the success of this effort, it is recommended that further research, development and engineering of the LLW method be continued to implementation of a versatile, commercially marketable bond testing system. Recommendations for specific areas of investigation within an overall development program include the following.

1. To date, theoretical analyses of the leaky Lamb wave phenomenon have not addressed practical concerns such as anisotropy and inhomogeneity of the adherends, geometrical effects, etc. This is an important area of further research. It is thus recommended that work to expand present modeling efforts be supported to provide practical guidance to the hardware development.

2. Various relationships between and interactions among parameters that affect the reliability of flaw detection and discrimination were revealed during the course of Phase I that could not be investigated in detail. An understanding of these relationships and interactions is essential to development of an optimized LLW system. Accordingly, it is recommended that further investigation and evaluation of the various parameter relationships receive major attention. It is likely that a significant--6 to 10 dB-- improvement in signal-to-background ratio can be achieved with greater understanding of the factors that affect the LLW method.

3. Detection and discrimination of flaws are highly dependent on how, and in what form, the results of an evaluation are displayed. It is therefore recommended that future work explicitly address the nature of the information provided by an LLW evaluation of a bond surface and the most effective way to present that information to maximize the reliability of flaw detection and discrimination.

REFERENCES

1. Chimenti, D. E., A. H. Nayfeh and D. L. Butler, J. Appl. Phys. 53, 170 (1982).

2. Nayfeh, A. H. and D. E. Chimenti, J. Acoust. Soc. Am. 75, 1360 (1984).

3. Chimenti, D. E. and A. H. Nayfeh, J. Appl. Phys. 58, 4531 (1985).

4. Chimenti, D. E. and Y. Bar-Cohen, "Signal Analysis of Leaky Lamb Wave Spectra for NDE of Composites," Proc. IEEE 1985 Ultrasonics Symposium, B. R. McAvoy (Ld.), (IEEE, New York, 1985).

5. Bar-Cohen, Y. and D. E. Chimenti, "Nondestructive Evaluation of Composites by Leaky Lamb Waves," Rev. Prog. Quant. NDE, Williamsburg, VA, June 1985.

6. Bar-Cohen, Y. and D. E. Chimenti, "NDE of Composite Laminates by Leaky Lamb Waves Using A Bubbler Device," Proc. 2nd Intl. Symp. Nondes. Charac. Mat., Montreal, Canada, July 1986.

7. Pitts, L. E., T. J. Plona and W. G. Mayer, J. Acoust. Soc. Am. 59, 1324-28 (1976).

8. Goos, F. and H. Haenchen, Ann. Phys. 1, 333 (1947).

9. Schoch, A., Acoustica 2, 18 (1952).

10. Schoch, A., Ergeb. Exakten Naturwiss. 23, 127 (1973).

11. Bertoni, H. L. and T. Tamir, Appl. Phys. 2, 157 (1973).

12. Pitts, Plona and Mayer, Ibid.

13. Ngoc, T. D. and W. G. Mayer, IEEE Trans. Sonics Ultrason, SU-27 229 (1980).

14. Mal, A.K., Personal Communication.

15. Kundu, T., A. K. Mal and R. D. Weglein, J. Acoust. Soc. Am. 77, 353-361 (1985).

16. Kundu T. and A. K. Mal, Int. J. Engr. Sc. 24, 1819-1829 (1986).

17. Mal, A. K. and R. Weglein, "Review of Progress in Quantitative NDE," D. O. Thompson and D. E. Chimenti (Eds.), (Plenum Press, NY, 1987).

18. Mal, A. K. and C.-C Tin and Y. Bar-Cohen, "Review of Progress in Quantitative NDE," D. O. Thompson and D. E. Chimenti (Eds.), (Plenum Press, NY, 1987).

ACKNOWLEDGEMENT

END

10-81

DTIC